SANDIA REPORT
SAND2013-8834
Unlimited Release
Printed October 2013

Brine-in-Crude-Oil Emulsions at the Strategic Petroleum Reserve

Martin B. Nemer, David L. Lord, Terry L. MacDonald

Prepared by
Sandia National Laboratories
Albuquerque, New Mexico 87185 and Livermore, California 94550

Sandia National Laboratories is a multi-program laboratory managed and operated by Sandia Corporation, a wholly owned subsidiary of Lockheed Martin Corporation, for the U.S. Department of Energy's National Nuclear Security Administration under contract DE-AC04-94AL85000.

Approved for public release; further dissemination unlimited.

Sandia National Laboratories

Issued by Sandia National Laboratories, operated for the United States Department of Energy by Sandia Corporation.

NOTICE: This report was prepared as an account of work sponsored by an agency of the United States Government. Neither the United States Government, nor any agency thereof, nor any of their employees, nor any of their contractors, subcontractors, or their employees, make any warranty, express or implied, or assume any legal liability or responsibility for the accuracy, completeness, or usefulness of any information, apparatus, product, or process disclosed, or represent that its use would not infringe privately owned rights. Reference herein to any specific commercial product, process, or service by trade name, trademark, manufacturer, or otherwise, does not necessarily constitute or imply its endorsement, recommendation, or favoring by the United States Government, any agency thereof, or any of their contractors or subcontractors. The views and opinions expressed herein do not necessarily state or reflect those of the United States Government, any agency thereof, or any of their contractors.

Printed in the United States of America. This report has been reproduced directly from the best available copy.

Available to DOE and DOE contractors from
U.S. Department of Energy
Office of Scientific and Technical Information
P.O. Box 62
Oak Ridge, TN 37831

Telephone: (865) 576-8401
Facsimile: (865) 576-5728
E-Mail: reports@adonis.osti.gov
Online ordering: http://www.osti.gov/bridge

Available to the public from
U.S. Department of Commerce
National Technical Information Service
5285 Port Royal Rd.
Springfield, VA 22161

Telephone: (800) 553-6847
Facsimile: (703) 605-6900
E-Mail: orders@ntis.fedworld.gov
Online order: http://www.ntis.gov/help/ordermethods.asp?loc=7-4-0#online

SAND2013-8834
Unlimited Release
Printed October 2013

Brine-in-Crude-Oil Emulsions at the Strategic Petroleum Reserve

Martin B. Nemer
Thermal Fluid Experimental Sciences Department

David L. Lord
Geotechnology and Engineering Department

Terry L. Macdonald
Repository Performance

Sandia National Laboratories
P.O. Box 5800
Albuquerque, New Mexico 87185-0346

Abstract

Metastable water-in-crude-oil emulsion formation could occur in a Strategic Petroleum Reserve (SPR) cavern if water were to flow into the crude-oil layer at a sufficient rate. Such a situation could arise during a drawdown from a cavern with a broken-hanging brine string. A high asphaltene content (> 1.5 wt %) of the crude oil provides the strongest predictor of whether a metastable water-in-crude-oil emulsion will form. However there are many crude oils with an asphaltene content > 1.5 wt % that don't form stable emulsions, but few with a low asphaltene content that do form stable emulsions. Most of the oils that form stable emulsions are "sour" by SPR standards indicating they contain total sulfur > 0.50 wt %.

ACKNOWLEDGMENTS

Thanks to Patrick V. Brady for performing a review of this work. Thanks to Collins Lanier, Lisa, Eldredge, and Pat Milhalik for their support of this work over the years.

CONTENTS

Acknowledgments 4

Contents 5

Figures 6

1 Introduction 9
  1.1 Background on Problem 9
  1.2 Literature Review 10
    1.2.1 Causes of Emulsion Stability – Asphaltenes, Resins, and Waxes 10
    1.2.2 Use of Bottle Tests 10

2 Initial Experiments on Big Hill Crude Samples 11

3 Characterization 13
  3.1 Crude Oil and Water Characterization 13
  3.2 Emulsion Characterization 14
    3.2.1 Emulsion Type 14

4 Impacts of Emulsion Formation 15
  4.1 Emulsion Rheology 15
  4.2 Roof Dissolution 16

5 Causes of Stability 19
  5.1 Polar Silica Test 19
  5.2 Asphaltene Solubility as a function of Temperature 20

6 Treatment Options 23
  6.1 Oil Based Emulsion Breaking Compounds 23
  6.2 Water Based Emulsion Breaking Compounds 24
  6.3 Oil Blending 27

7 Flow Conditions Required to Form Stable Emulsion 29
  7.1 Well-Head Sampled BH106 Crude Oil Experiments in the Small-Scale SPR Tank 29
    7.1.1 Experimental Methodology 32
    7.1.2 Runs Performed 36
    7.1.3 Results 37
  7.2 Recovery Times and Stable Emulsion Formation 38

8 Bottle Tests on All SPR Oils 40

9 Conclusions 45

References 47

Appendix A. Complete Oil Blending Experimental Data 49

Appendix B: Full downhole-Sampled Crude oil Bottle Test Results with Time 52

Appendix C: New Mexico Tech Report 66

Samples 66

Experimental Methods 66
Physical Properties 66
Chemical Characteristics 67
Interfacial Tensions 67
Results 67
References 70
Distribution 71

FIGURES

Figure 1. Schematic of normal and broken string configurations. 9
Figure 2. Confocal microscope image of a stable raw-water-in-crude-oil emulsion). 14
Figure 3. Stable BH112 emulsion obtained at two different Reynolds numbers. 16
Figure 4. Image of the mother emulsion used for the salt-dissolution experiments. 17
Figure 5. Image of a bottle containing 5 g of halite and 30 g of emulsion. 18
Figure 6. Bottle tests of Big Hill Cavern 112 well-head-sampled oil. 20
Figure 7. Cross-Polarized images of BH101, and BH112 + nonane at temperature. 21
Figure 8. Stable emulsion formed from well-head-sampled BH112 oil. 23
Figure 9. Separated SPR crude-oil emulsion using Nalco Ultrion 8186 25
Figure 10. Gas Chromatograph of gases flashed off aqueous portion of separated emulsion. 26
Figure 11. Series of blended oil experiments using.. 28
Figure 12. Schematic of the small-scale SPR tank setup. 30
Figure 13. Image of small-scale-tank setup 31
Figure 14. Drop-size (diameter) distribution for a stable emulsion 33
Figure 15. Sequence of steps in a SPR small-tank experiment. 35
Figure 16. Image of stable-brine-in-crude-oil emulsion from small-tank experiment. 37
Figure 17. Fraction of brine that becomes entrained in the crude oil during flow of brine into the crude oil. 38
Figure 18. Time required for the unstable black-brine-in-oil interface to return to its original height. 39
Figure 19. Asphaltene wt % versus vol_{water} %.. 41

TABLES

Table 1. Big-Hill Well-Head Oil Sample Lab Emulsion Stability Tests. 11
Table 2. Well-Head Big Hill Crude Oil Physical Properties 13
Table 3. Well-Head Big Hill Crude Oil Chemical Properties 13
Table 4. Viscosity of two well-head-sampled BH112 stable emulsions 15
Table 5. Asphaltene Dissolution Test Results 20
Table 6. Summary of blended oil experiments. 27
Table 7. Parameter values used in this report. 33
Table 8. Comparison of experimental flow parameters to those applicable to SPR..... 34
Table 9. List of runs performed using the small-scale SPR tank.. 36
Table 10. Bottle test results for downhole-sampled SPR oils..... 42
Table 11. List of caverns that do not have a bottle test result..... 43
Table 12. Raw data from the blended oil experiments. 49

NOMENCLATURE

dB	decibel
DOE	Department of Energy
SNL	Sandia National Laboratories
Re	Reynolds number
NMT-PRRC	New Mexico Tech Petroleum Research and Recovery Center
SPR	Strategic Petroleum Reserve
API	American Petroleum Institute gravity
cP	centi-poise
RI	refractive index

1 INTRODUCTION

1.1 Background on Problem

This study addresses whether raw-water[1] injection through a broken hanging string will cause a stable emulsion to form, and what will be the impact on SPR. A schematic drawing of the normal and broken string configurations are shown in Figure 1. Water injection through the broken hanging string would expose the oil to a high-volume-flow-rate jet of raw water, through a distance from the end of the hanging string to the brine layer below. This energetic commingling of immiscible phases in the presence of natural surfactants from the oil has the potential to form stable dispersions of water in oil, which is called an emulsion. The presence of the "sludge" layers in SPR caverns is a realization of the potential to form such stable configurations, although it is unclear how existing sludge layers formed. Emulsions have the potential to adversely affect oil quality by introducing water into the oil at a concentration greater than delivery requirements. The viscosity of the emulsion is too high to flow up through the oil string.

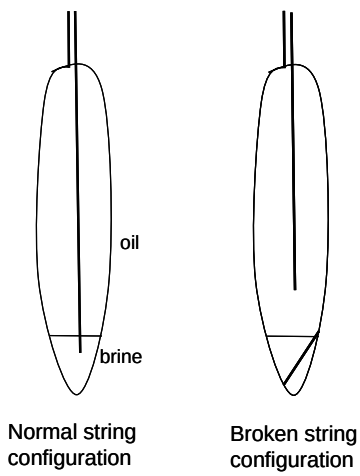

Figure 1. Schematic of normal and broken string configurations.

When two immiscible fluids are mixed together in a shearing flow, one phase will become the continuous phase and the other will become the dispersed phase. When drops of the disperse phase undergo shear flow, the strain component of the shear flow stretches the drops in the strain direction. If this straining stress is greater than the surface-tension restoring stress on the drop, the drop will break into two or more smaller drops. This continues until the drops are small enough so that the straining stress is less than the surface-tension stress.

[1] Raw water in the context of the Strategic Petroleum Reserve is surface water, fresh or brackish, that is picked up by the raw water intake structure, and used to displace oil from a cavern during a drawdown operation.

1.2 Literature Review

1.2.1 Causes of Emulsion Stability – Asphaltenes, Resins, and Waxes

It is known that small solid-like particles of asphaltene, resin, and wax can stabilize water-in-crude-oil emulsions (Lee, 1999, Sjoblom, et al., 1992, McLean and Kilpatrick, 1997, Spiecker, et al., 2003) by sterically preventing drop coalescence. However it is also possible that the equilibrium concentration of asphaltene absorbed onto the water-oil interface determines emulsion stability (Kilpatrick, 2012). In either case, determining the total fraction of asphaltene, resin, and wax in an oil sample is not thermodynamically sufficient to predict whether the oil will form a stable emulsion (Eley, et al., 1988), because one needs to know how much asphaltene is precipitated as a solid and how much will absorb to the water-oil interface (Gafonova and Yarranton, 2001). Further complicating the picture, asphaltenes are not a monolithic block of compounds; some stabilize emulsions and some destabilize emulsions (Kilpatrick, 2012). These compounds exist over a wide spectrum of molecular structures, and thus chemical analyses of their individual concentrations are difficult if not impossible.

1.2.2 Use of Bottle Tests

Emulsion bottle tests are performed by pouring equal amounts of water and oil into a small bottle and then shaking the mixture vigorously. If the two immiscible fluids separate within a reasonable amount of time (few days), then it is concluded that the system does not form a stable emulsion. If the two fluids do not separate, it is concluded that the system is capable of forming a stable emulsion. Although the test is simple in execution, it remains the industry standard. Poindexter et al. (2005) of Nalco Chemical Co. used emulsion bottle tests to correlate crude-oil emulsion stability to asphaltene, solids, resins, and wax content in the crude oil. Pena et al. (2005) of Rice University used emulsion bottle tests to examine the efficacy of commercial emulsion-breaking compounds on crude-oil emulsions. Thompson et al. (1985) of BP used emulsion bottle tests to examine at the effect of waxes on crude-oil emulsion stability. Goldszal and Bourrel (2000) of ELF France used emulsion bottle tests to optimize the amount emulsion-breaking compounds needed to breakup crude-oil emulsions. Fan et al. (2009) of the Norwegian University of Science and Technology used bottle tests to examine the use of nonionic surfactants as emulsion-breaking compounds for treating crude-oil emulsions.

2 INITIAL EXPERIMENTS ON BIG HILL CRUDE SAMPLES

Initial bottle tests were performed by Sandia on crude-raw water samples from 13 caverns at Big Hill. In each bottle 15 mL of crude oil was mixed with 15 mL of raw water. The bottles were then shaken by hand vigorously for 1 minute. When a stable emulsion formed, the water content of the emulsion was on the order of 50 vol % which exceeds the SPR oil quality requirements of 1.75 vol % (U. S. Department of Energy, 2004). The crude oil and brines for these tests were obtained from the Big Hill well heads. Bottle tests on downhole-sampled SPR cavern oils were performed by DynMcDermott as discussed in Section 8, however there are differences between the two sets of results; in particular the Sandia results showed that BH111 and BH112 form a stable emulsion, whereas the results obtained from DynMcDermott did not show a stable emulsion.

Table 1 shows the results of the bottle tests on well-head Big Hill oils including whether an oil formed a stable emulsion, previous asphaltene testing by DynMcDermott, and asphaltene testing by the New Mexico Tech – Petroleum Resource Research Center (NMT-PRRC, see Section 3.1). As can be seen from Table 1, the formation of a stable emulsion was highly correlated with the asphaltene testing performed by NMT-PRRC, i.e. higher asphaltene content (~ 3 wt %) lead to stable emulsions. Table 1 also shows that the SPR asphaltene testing is consistently below that of NMT-PRRC for every sample tested, although the two results are highly correlated (R^2 = 0.96).

Table 1. Big-Hill Well-Head Oil Sample Lab Emulsion Stability Tests.

Cavern	Stable Emulsion Formed in Lab	n-C6 Asphaltenes[2] (wt %)	Asphaltenes previous analysis[4] (wt %)
101		1.2	0.33
102		1.7	1.1
103		0.9	0.26
104		1.2	0.35
105		1.1	0.54
106	X	3.1	2.1
107	X	3.4	2
108	X[3]	3.1	1.9
109			NA
110			NA
111	X	2.4	1.57
112	X[1]	3.0	1.79
113			1.77
114			0.37

1. In one test the sample separated slightly, in a second test it did not separate.
2. Measured by NMT-PRRC see Section 3.1
3. Partially separated.
4. Taken from SPR Crude Oil Comprehensive Analyses performed by Dyne McDermott.

3 CHARACTERIZATION

3.1 Crude Oil and Water Characterization

Sandia contracted with New Mexico Tech Petroleum Recovery Research Center (NMT-PRRC) to analyze 10 well-head-sampled Big Hill crude-oil samples, cavern brines, and Big Hill raw intake water. A full copy of the report is included in Appendix B. Here we only summarize the most salient features of the report. Table 2 shows the density, viscosity and refractive index of well-head Big Hill oils. Table 3 shows the acid and base numbers, and the weight percent of saturates, aromatics, resins, and asphaltenes, also known as a SARA analysis. The sour oils have viscosities and asphaltene concentrations that are generally double those of the sweet oils.

Table 2. Well-Head Big Hill Crude Oil Physical Properties (Table 2. in NMT-PRRC report)

Oil	density at 20ºC (g/cm^3)	°API	viscosity at 20ºC (cP)	RI	Sweet/Sour
101	0.8385	36.6	5.23	1.4707	Sweet
102	0.8457	35.2	5.82	1.4748	Sour
103	0.8408	36.2	5.23	1.4717	Sweet
104	0.8349	37.4	5.20	1.4693	Sweet
105	0.8344	38.1	4.96	1.4693	Sweet
106	0.8618	32.7	10.06	1.4867	Sour
107	0.8597	32.5	9.93	1.4858	Sour
108	0.8621	32.0	10.17	1.4870	Sour
111	0.8535	33.7	7.95	1.4804	Sour
112	0.8707	30.4	14.23	1.4911	Sour

Table 3. Well-Head Big Hill Crude Oil Chemical Properties (Table 3. in NMT-PRRC report)

Oil	Acid #	Base #	Saturates	Aromatics	Resins	n-C6 Asphaltenes
	mg KOH/g oil		wt %			
101	0.30	1.56	66.3	19.9	12.6	1.2
102	0.49	2.55	62.2	19.4	16.7	1.7
103	0.43	1.71	64.3	21.4	13.5	0.9
104	0.19	1.47	64.0	21.9	13.0	1.2
105	0.20	1.47	64.5	20.5	13.9	1.1
106	0.28	1.44	59.5	21.3	16.2	3.1
107	0.28	1.46	58.2	21.6	16.8	3.4
108	0.29	1.50	58.3	21.6	17.0	3.1
111	0.43	1.57	59.7	23.8	14.1	2.4
112	0.30	1.65	56.3	21.8	18.9	3.0

3.2 Emulsion Characterization

3.2.1 Emulsion Type

To determine whether the metastable emulsions formed are water-in-oil or oil-in-water type, emulsions of well-head-sampled Big Hill crude oil and raw intake water were prepared and imaged using an Olympus petrographic microscope under transmitted light. We also wanted to determine whether significant quantities of air were being entrained as small bubbles in our experiments. Entrained air would have been an experimental artifact since we do not anticipate a gas phase around a broken brine string hanging in the oil phase. In this experiment we placed equal amounts (15mL) of well-head-sampled Big Hill cavern 112 oil into a small bottle. The aqueous phase was dyed with methylene blue (60 mg dye to 15mL water); methylene blue is not soluble in the oil phase. The bottle was then shaken vigorously. A small sample of the emulsion was taken, placed on a glass slide and imaged, as shown in Figure 2. Given the blue dispersed phase and the dark brown continuous phase it is reasonable to conclude that this emulsion is a water-in oil type, although a small fraction of the dispersed phase does appear clear. Particulate can be seen in some blue drops, this is un-dissolved methylene blue. The drop radii are ~ 3 – 250 μm.

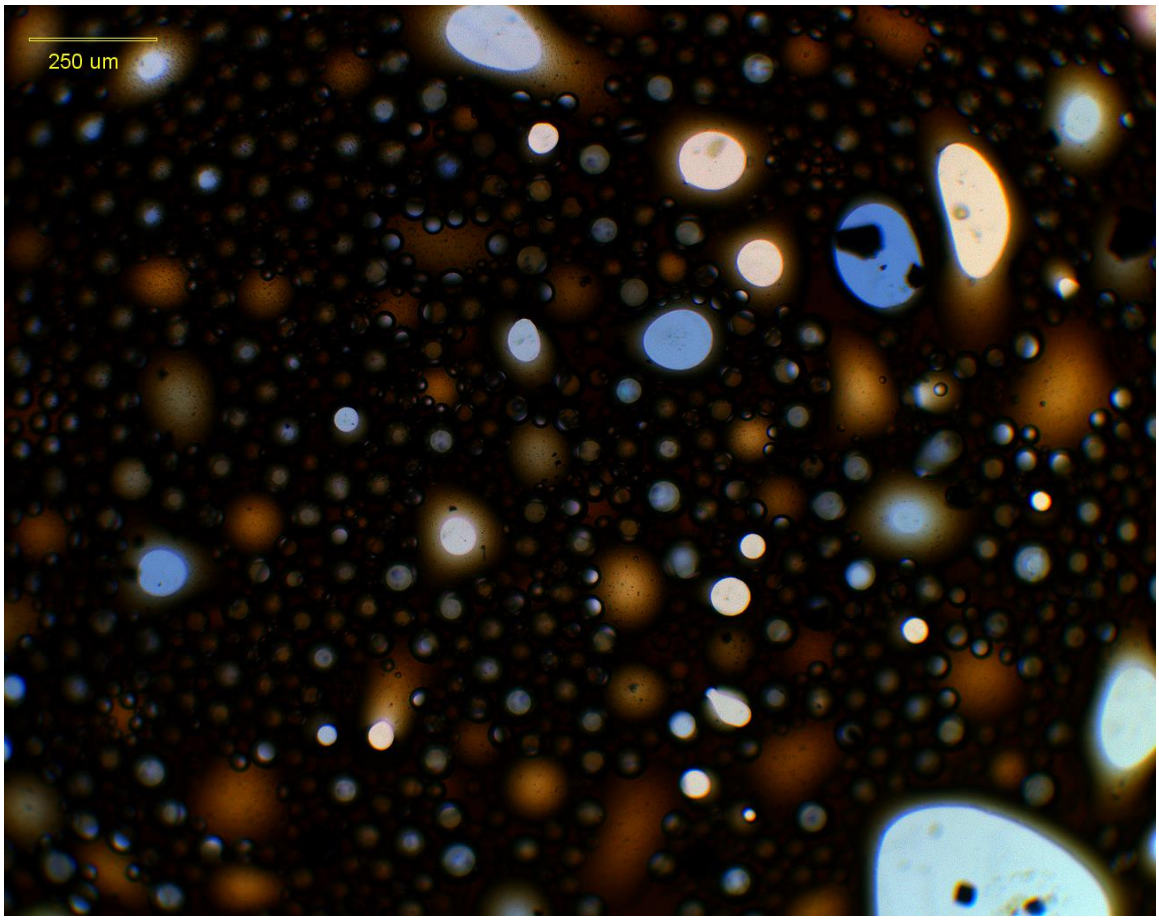

Figure 2. Confocal microscope image of a stable raw-water-in-crude-oil emulsion prepared from Big Hill raw intake water and cavern-107 well-head-sampled Big-Hill oil. The water phase was dyed with a blue dye (methylene blue).

4 IMPACTS OF EMULSION FORMATION

4.1 Emulsion Rheology

The rheology of two stable emulsions made from well-head-sampled BH112 oil and raw intake water were tested to obtain basic viscosity versus shear rate data. The emulsion was prepared at two Reynolds (Re) numbers, sample A = 92,000 and sample B = 184,000, in a turbulent mixing tank. Although qualitative, the results illustrate the effects of strong turbulent flow on SPR oil emulsion formation and rheology. Images of the two emulsions are shown in Figure 3. Both emulsions are brown colored with the higher Re emulsion being lighter in color. The thick tooth-paste like emulsion was scooped out of each bottle and placed into the Fann viscometer. Both emulsions were shear thinning, and show considerable hysteresis as a function of shear rate. The viscosity as a function of shear rate is given below in Table 4 for the two samples. The viscosity of well-head-sampled BH112 oil at 25 °C is 12 cP (see Section 3.1). Thus the emulsion has a viscosity on the order of 10-20 times that of the crude oil.

We expected that sample B would have a higher viscosity than sample A since it was produced under stronger shear conditions. A large source of error is that we scooped the emulsion out of the bottle which caused some un-emulsified oil to end up in the viscometer.

Table 4. Viscosity of two well-head-sampled BH112 stable emulsions as a function of shear rate at 25 °C ± 2 °C.

Shear Rate (sec^{-1})	Viscosity of Sample A (cP)	Viscosity of Sample B (cP)
5.1	900	600
10.2	800	300
170	441	285
340	364.5	213
511	NA	200
1021	NA	NA

NA indicates that the shear stress was above full scale on the Fann 35 viscometer.

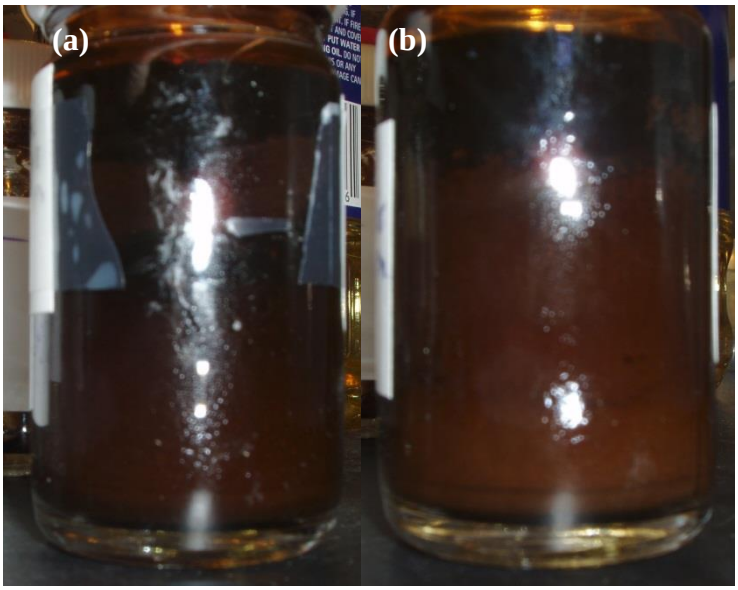

Figure 3. Stable BH112 emulsion obtained at two different Reynolds numbers, (a) Sample A: Re = 92,000, (b) Sample B: Re = 184,000. Notice that the color of (b) is a lighter than (a), indicating a smaller drop size.

4.2 Roof Dissolution

A set of experiments was conducted to investigate the ability of an unsaturated brine-in-crude-oil emulsion to dissolve roof halite; to determine whether an emulsion layer is capable of dissolving the roof of a cavern. In these experiments we began by forming a stable water-in-crude oil emulsion using equal parts de-ionized water (DI, 125 ml) and well-head-sampled crude oil (125 ml) from Big Hill cavern 111, and shaking together in a 250 ml bottle for two minutes. Figure 4 shows a picture of this emulsion taken on 9/21/2008 (i.e. at the end of the experiment). Next 30 grams (approximately 30 ml) of this emulsion was poured into smaller 40 mL bottles, each containing 5 grams of previously-weighed pure-dry halite (NaCl, Fisher ACS grade). The bottles were closed and put onto a shelf where they were not shaken or otherwise disturbed (on 9/3/2008). Eighteen days (9/21/2008) later the bottle containing the stock emulsion and the bottle containing the emulsion plus salt were photographed, as shown in Figure 4 - Figure 5. What is clear from Figure 4 - Figure 5 is that that little to no water has separated out of the stock emulsion, while it appears that the salt drew water out of the emulsion, causing salt dissolution. We were unable to determine the mass of halite that dissolved. The halite layer contains oil and tar that stuck to it, which was difficult to wash off with hydrocarbon solvents. In the oven, upon drying at ≈ 100 °C, the salt decrepitated and much of the mass escaped the crucible and wasn't recoverable. Another interesting observation was that a small layer of crude oil remained trapped between the brine and the emulsion. The hydrostatic head may be insufficient for this oil to flow through the plateau borders separating the water droplets, i.e. not enough pressure to push the oil back to the top of the bottle.

Figure 4. Image of the mother emulsion used for the salt-dissolution experiments, taken on 9/21/2008; the emulsion was prepared on 9/3/08 and remained stable throughout the experiment. There is a visible layer of free oil at the top of the liquid that has been squeezed out of the emulsion by capillary pressure and gravity.

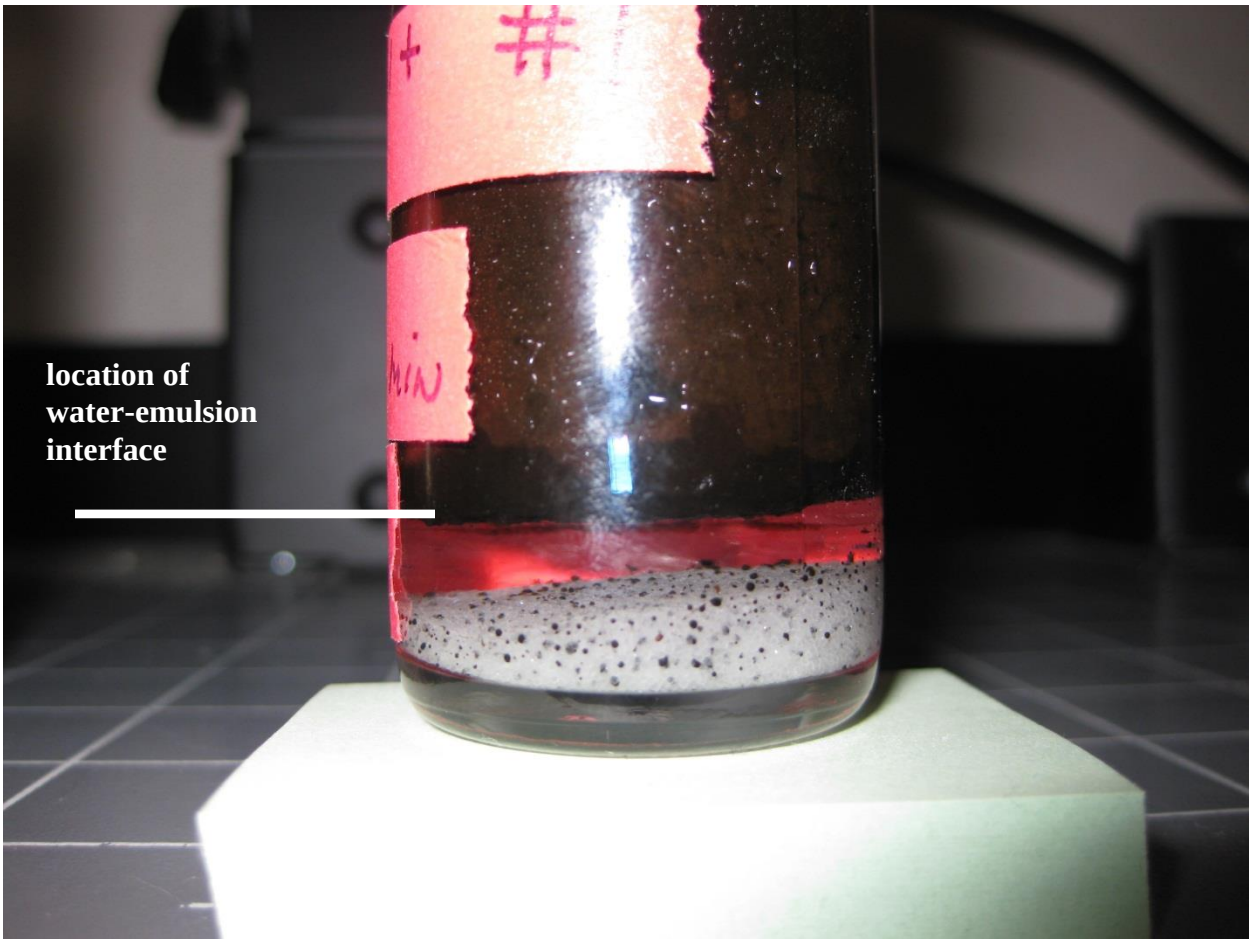

Figure 5. Image of a bottle containing 5 g of halite (NaCl, Fisher ACS grade), and 30 g of emulsion (shown in Figure 4) created from Big Hill cavern 111 well-head-sampled oil and DI water. The emulsion has separated in the vicinity of the halite causing local halite dissolution, leaving a local layer of oil "trapped" between the brine and the emulsion.

5 CAUSES OF STABILITY

5.1 Polar Silica Test

It is well known that asphaltenes and other polar compounds that naturally occur in crude oil are often primarily the cause of problem emulsions in the oil field (Fingas and FieldHouse, 2003). Asphaltenes are more polar than alkanes and tend to stick to the oil-water interface. Because of their large molecular size asphaltenes sterically inhibit drop coalescence, either by sterically inhibiting drops from getting close enough to coalesce or by making the drop interface rigid (incompressible surface) such that coalescence is not favorable. Sjoblom et al. (1992) developed a simple test to determine whether polar compounds in the oil are the cause of emulsion stability in water-in-crude emulsions. In this test the asphaltenes and other polar compounds are chemically removed from the oil by absorbing them onto polar silica. The oil is then re-tested to determine whether it can form a stable emulsion.

In this experiment, five grams of silica beads (US Silica cat# MIN-U-SIL 5B) were added to a beaker. Ten ml of well-head sampled BH112 crude oil was added and n-hexane (Acros ECD grade) was added to dilute to 100 ml. The beaker was gently stirred and then the liquid was filtered with Whatman #42 filter paper. The silica was discarded and the procedure repeated until the silica beads no longer appeared brown. The liquid was then filtered using a 0.45 μm syringe filter into a clean beaker and heated to evaporate off the hexane and return the oil to its original 10 ml volume. The reduced oil was then mixed with 10 ml of brine and shaken for one minute. No stable emulsion was formed from the treated oil, whereas untreated well-head-sampled BH112 oil formed the most stable emulsions of the well-head-sampled Big Hill cavern oils tested. This is illustrated in Figure 6; the final condensed oil is still a dark brown color, although slightly lighter in color than the original oil.

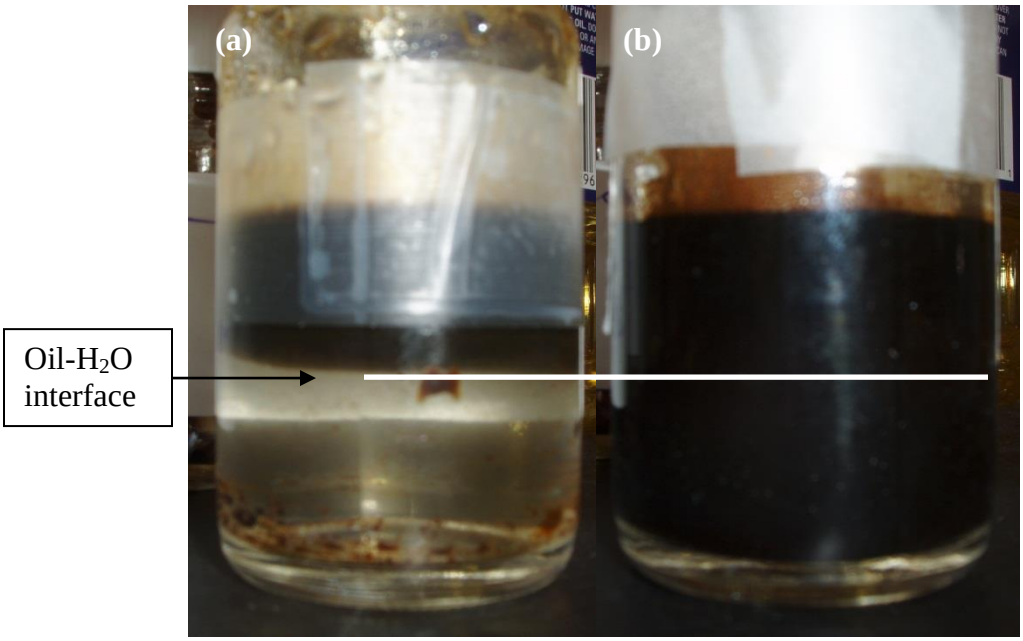

Figure 6. Bottle tests of Big Hill Cavern 112 well-head-sampled oil; (a) bottle test using BH112 oil after removing the asphaltenes and other polar compounds from the oil (several minutes after mixing); (b) bottle test on un-treated BH112 oil (several days after mixing). The white line represents where the oil-brine interface should be upon complete separation.

5.2 Asphaltene Solubility as a function of Temperature

Because the typical SPR cavern temperature is roughly 50 °C, one question that has been asked is whether room-temperature lab experiments are relevant, given that the asphaltene solubility in the oil increases with temperature. The idea is that the asphaltene is thermodynamically less driven to the water-oil interface as its solubility increases in the oil phase. To test this hypothesis, NMT-PRRC tested two Big Hill well-head-sampled oils, BH101 and BH112, to determine the asphaltene solubility in the crude oil as a function of temperature. In this test nonane (C_9H_{20}) was first added to the crude oil until solids were seen to precipitate out of solution, as viewed on a heated microscope stage under cross-polarized light. Next the sample was heated to view the temperature at which the asphaltene solids dissolve back into solution. The results are shown in Table 5. The sequence of images used to determine the dissolution temperatures are shown in Figure 7. Consequently a sample of BH112 emulsion made from BH112 oil and brine was heated to 60 °C for several hours to see if it would separate; no evidence of separation was observed.

Table 5. Asphaltene Dissolution Test Results

Sample	Oil to nonane (vol/vol)	Dissolution temperature (°C)
BH101	52/48	60
BH112	68/32	60

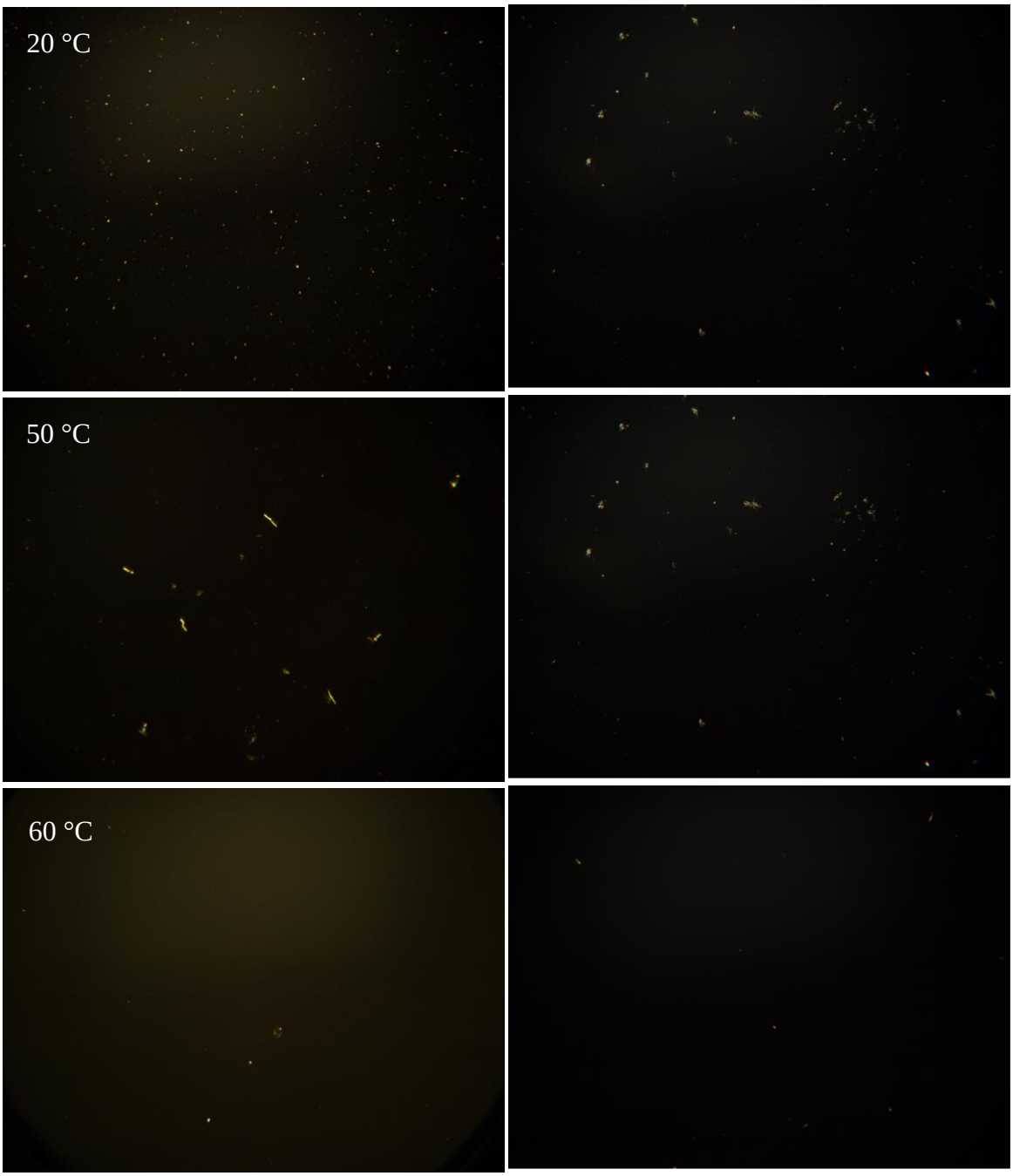

Figure 7. Cross-Polarized images of BH101 (left), and BH112 (right) + nonane (volumes given in Table 5) at 20 °C, 50 °C and 60 °C.

[This page intentionally left blank]

6 TREATMENT OPTIONS

6.1 Oil Based Emulsion Breaking Compounds

Experiments were performed to determine whether commercial oilfield de-emulsifying chemicals (Nalco) might be able to either prevent or break a stable SPR crude-raw water emulsion. One of the Nalco de-emulsifying chemicals was tested on a stable emulsion, prepared from well-head-sampled BH112 oil, shown in Figure 8a. Nalco de-emulsifying compound EC2063A was added to the stable emulsion to a final concentration of 3000 ppm (as per Nalco instructions). Within 5 hours the emulsion had separated considerably, as shown in Figure 8b but also induced considerable cloudiness of the water phase in Figure 8b. This is likely due to colloidal organic micelles suspended in solution composed of the de-emulsifying compound and heavy aromatics. In oilfield applications, the brine is normally disposed of in existing wells or reused, unlike SPR where the brine is typically discharged. Thus the use of these chemicals could generate a discharge-permit issue.

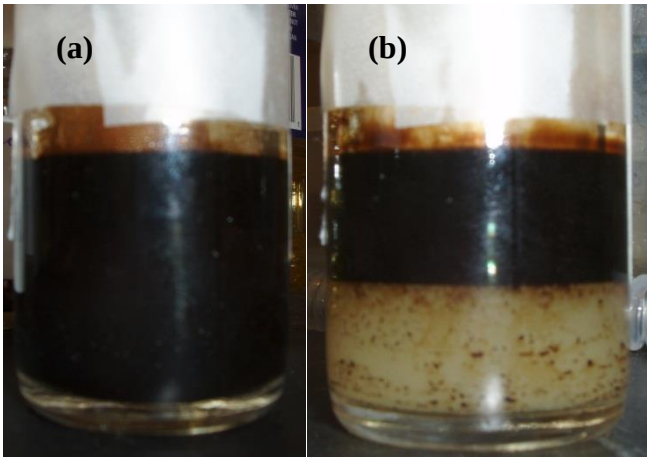

Figure 8. Stable emulsion formed from well-head-sampled BH112 oil (a) before adding de-emulsifying compound, (b) five hours after adding 0.1 mL of Nalco de-emulsifier EC2063A.

In a separate experiment, Nalco EC2063A was added to well-head-sampled BH112 oil prior to emulsification, to determine whether a significant reduction in separation time could be achieved, relative to the experiment described in the previous paragraph. We did not observe a significant reduction in the separation time compared to the experiment explained in the paragraph above. In this later experiment, a cloudy colloidal water layer after separation was also observed.

6.2 Water Based Emulsion Breaking Compounds

Nalco Chemical Co. was given a sample of raw-water-in-crude-oil emulsion that was prepared in our lab. This was accomplished by mixing roughly equal parts of Big Hill Cavern 112 well-head-sampled oil with Big Hill raw-intake water. The total volume was about 1 liter. The bottle was shaken vigorously for several minutes and allowed to sit. Over the next few days the bottle was repeatedly shaken for several minutes to ensure that the sample sent to Nalco would be sufficiently difficult to separate. Nalco then added their emulsion breaking compound, Ultrion 8186, at a concentration of 20 parts per million. The sample was then centrifuged which caused to the emulsion to separate with a clear aqueous later, as shown in Figure 9. Nalco also ran a qualitative analysis of the separated water which is shown in Figure 10. Aromatics and other regulated compounds are present, but the concentrations of these compounds in the aqueous phase would have to be compared with the equilibrium concentrations between the crude oil and raw water, i.e. their presence may not be related to the emulsion-breaking compound. Further testing and quantitative brine analysis by a certified laboratory should be performed to be able to show that the brine meets disposal requirements. Further testing and quantitative analysis of the oil would also be required to ensure that the compound doesn't affect oil quality requirements.

Figure 9. Separated SPR crude-oil emulsion (BH112 well-head oil and BH raw-intake water) using Nalco Ultrion 8186 at a concentration of 20 ppm. This experiment was performed by Nalco chemical company using an emulsion that SNL prepared. The resulting aqueous layer appears clear unlike that obtained using oil-based emulsion breaking compounds.

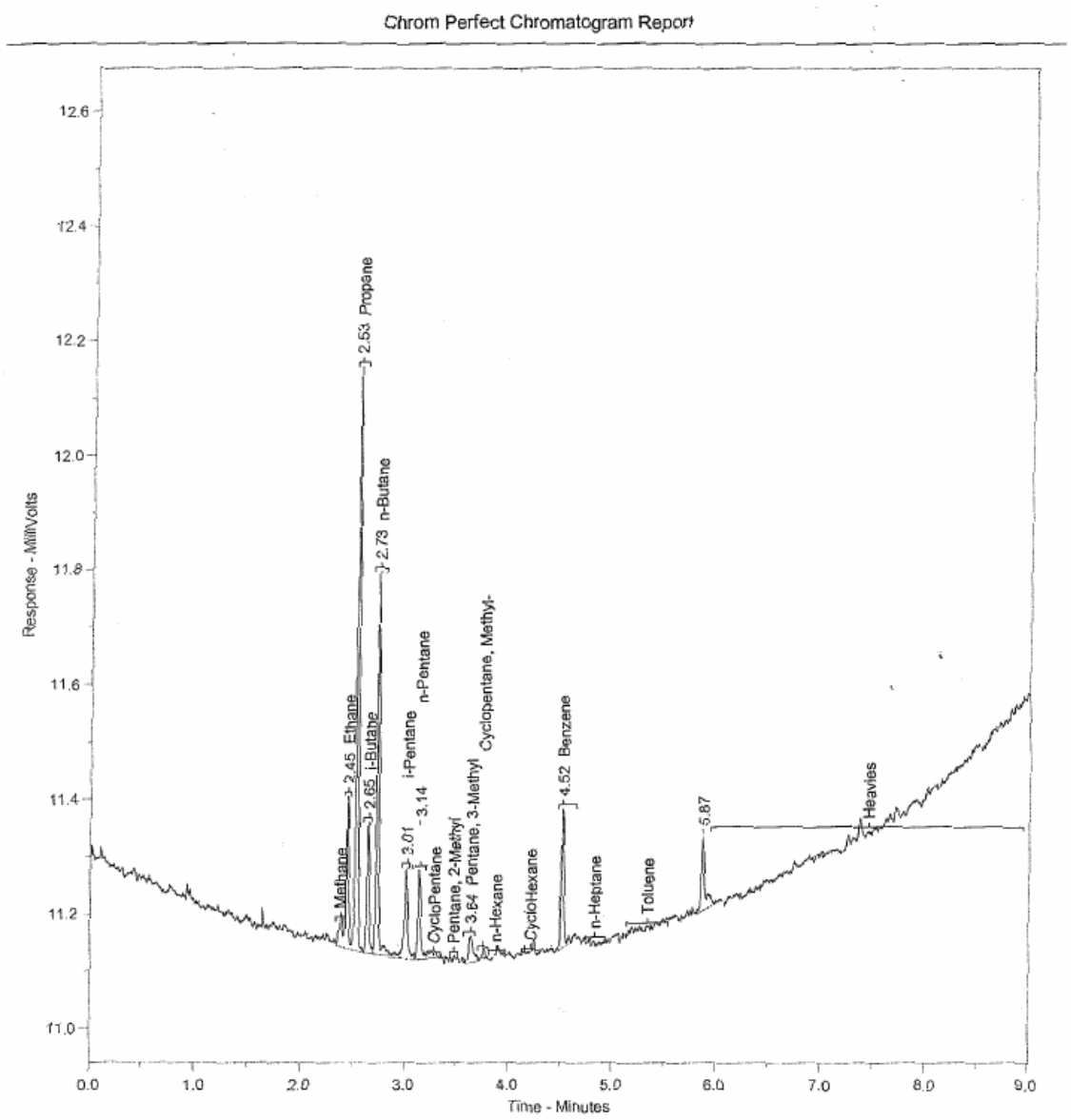

Figure 10. Gas Chromatograph of gases flashed off aqueous portion of separated emulsion shown in Figure 9.

6.3 Oil Blending

We investigated the idea of blending oils from two separate caverns with a high and low asphaltene concentration to produce a new oil that would not form a stable emulsion. In this experiment, the two oils were mixed for a total volume of 15 mL, and adding the mixture to 15 mL of raw-intake water (saline but not saturated brine) in a bottle. The bottles were then hand shaken vigorously for two minutes and re-shaken in some cases. All of the oils were well-head Big-hill samples. The results of this experiment are shown in Table 6. In Table 6, the yellow columns give the cavern id, the volume and the wt % asphaltene for the high-asphaltene oils used, and the turquoise columns gives the same information for the low-asphaltene oils used. The volume of oil A in Table 6 is the minimum volume of oil A required to form a fully-stable emulsion, i.e. little or no water had separated from these systems after mixing. The resulting asphaltene concentration of the mixture is shown in the white column, calculated by volume averaging the asphaltene wt % of oils A and B. The average and standard deviation of the calculated asphaltene concentration of the stable systems is also given. According to Table 6, any blend that has an asphaltene content above ~ 1.7 wt % had a high potential for forming stable water-in-crude emulsions. Thus, for example, down-blending cavern 112 with cavern 101 to an asphaltene content of 1.5 wt % (at which we would expect little emulsion to form) would require the volumetric oil makeup of the final cavern to be 83 % from cavern 101 and 17 % from cavern 112.

Table 6. Summary of blended oil experiments showing asphaltene concentration (wt %) required to fully stabilize the emulsion.

Oil A Sample ID	Vol (mL)	Asphaltene (wt %)	Oil B Sample ID	Vol (mL)	Asphaltene (wt %)	Oil A + Oil B Asphaltene (wt %)
CAV106 A	3.5	3.1	CAV101A	11.5	1.2	1.64
CAV106 A	5	3.1	CAV105A	10	1.1	1.77
CAV108A	6	3.1	CAV103A	9	0.9	1.78
CAV111A	8	2.4	CAV103A	7	0.9	1.70
					Average:	1.72
					Standard deviation:	0.07

Table 6 is subjective because many oils show a “grey” area where the system is partially emulsified with some free water at the bottom; the full set of experimental observations is given in Appendix A, Table 12. Figure 11 illustrates this “grey” behavior and the difficulties that we have encountered in interpreting these experiments and in interpreting the mixing experiments. In the figure, well-head-sampled oils from Big Hill caverns 108 and 102 were blended together in various ratios (given in the figure). Instead of a sharp cut off between stable and unstable emulsification, we see a gradation in the amount of water that has separated as a function of the net asphaltene content of the oil. This is not surprising given that cavern 102 has an asphaltene wt % of 1.7 which is close to the emulsion stability boundary given in Table 6. A more useful metric might be the amount of free oil (i.e. oil that doesn’t contain a significant amount of water) that separates at the top of the mixture after a known amount of time.

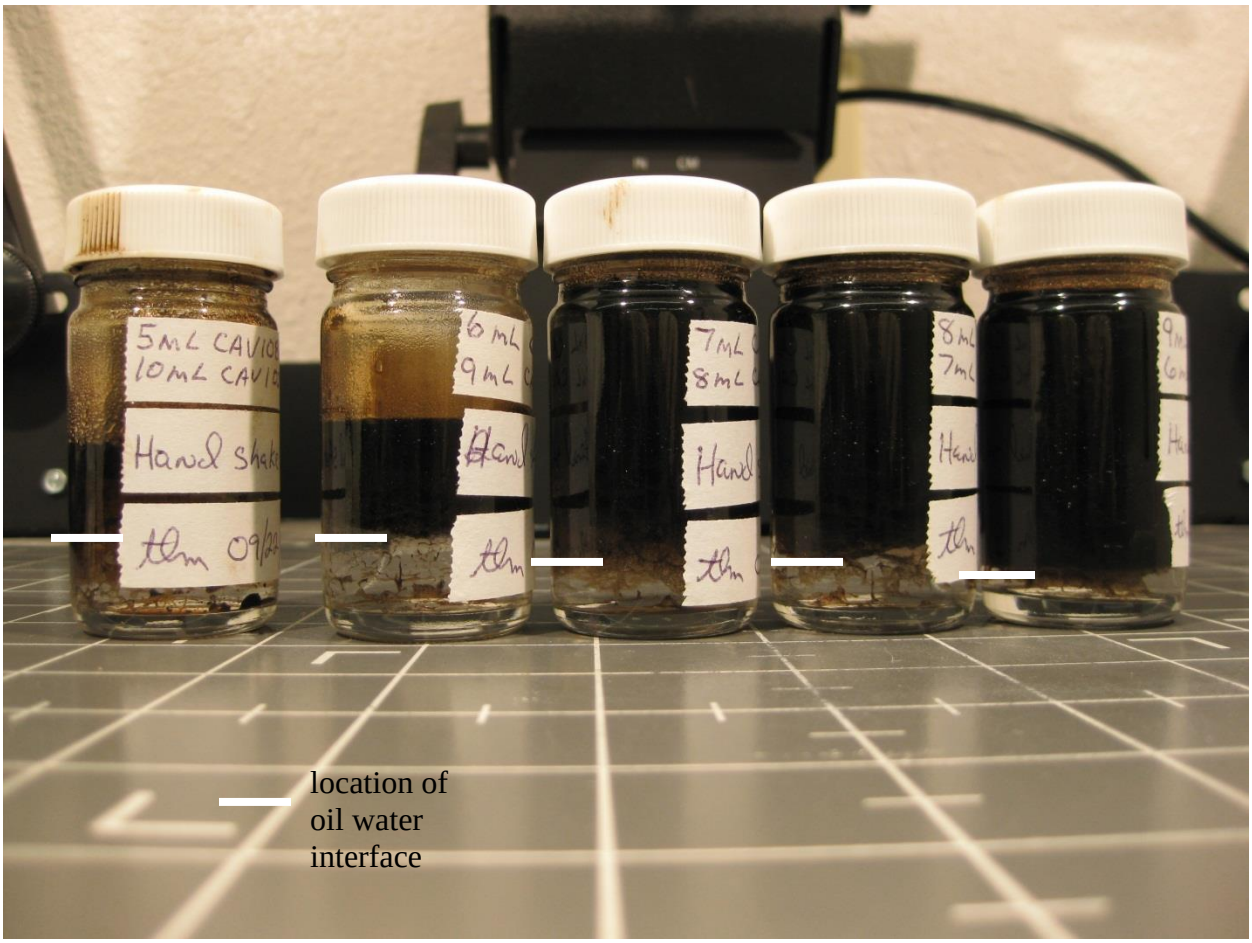

Figure 11. Series of blended oil experiments using well-head-sampled oils from Big Hill caverns 108 and 102. In each bottle in the figure the top number (i.e. 5 mL for the leftmost bottle) is the volume of oil from cavern 108, and the lower number is the volume from cavern 102. The amount of free water visible in the bottom of the bottles (white bar marks the oil-brine interface) decreases as the amount of cavern 108 oil is increased (which increases the asphaltene concentration of the oil). In the first two left-hand bottles the free (separated) oil has been removed and weighed, hence the headspace at the top of the bottles.

7 FLOW CONDITIONS REQUIRED TO FORM STABLE EMULSION

7.1 Well-Head Sampled BH106 Crude Oil Experiments in the Small-Scale SPR Tank

A bench-scale mockup of an SPR cavern was built to examine the effects of geometry on brine-in-crude-oil emulsion formation at SPR. The idea of these experiments was to flow brine through a jet pointing downward into the upper portion of the tank containing crude oil and/or an oil surrogate. The goal was to determine the flow rates required to form a stable emulsion due to the brine jet and scale these up to SPR conditions using standard dimensional analysis (Barenblatt, 1996).

A schematic of the small-scale tank is shown below in Figure 12. In this design a 4-inch-inner-diameter 23-inch-long acrylic tube is connected to two end caps. Drilled through the center of the top end cap is a ¾ inch diameter port through which a ¾ inch diameter stainless-steel tube runs. The stainless-steel tube represents the hanging brine string. The tube height is adjustable from close to the bottom to the top of the tank. At the bottom of the stainless-steel tube is a jet orifice. The available jet diameters are 1/8 in, 1/4 in, 3/8 in, 1/2 in, and 3/4 in. At the bottom of the tank is a 3/4 inch drain that connects to a pump. The pump (Iwaki Magnetic Pump, model MD-70RLZ7, max flow rate 11.4 gal/min, max head 66 ft) is connected to a flow meter (Endress + Hauser Promag P, model 50P15-EL0A1AA0B4AD) and a one-way valve for shutting off the flow. A rheostat (Staco Energy Prod. Co., 0-140 V, 10 Amp, model 3PN1010B) controls the flow rate by altering the voltage to the pump. The top cap of the small-scale tank contains a second port for sampling the emulsion and for sending logging tools into our small-scale cavern. A yellow tape measure is affixed to the outside of the tank for recording the oil-brine interface height versus time. A JVC Everio HD video camera is used to record video of each flow test. A photograph of the setup containing 5 m NaCl and Big Hill (BH) cavern 106 crude oil is shown in Figure 13.

The results of this study indicate that the critical velocity needed to produce a stable emulsion decreases with increasing jet diameter, as was expected. For a 3/8 inch nozzle diameter the critical velocity needed to form a stable emulsion was ≈ 12.3 ft/sec (3.7 m/sec), which is very close to a drawdown velocity encountered at SPR 11.7 ft/s (3.6 m/sec) (i.e. 95,000 bbl/day through a 9.85 in pipe). Based on these results, we believe it is unlikely that an operationally-relevant flow rate could be found that would prevent permanent emulsification in a real SPR cavern, if brine (or brackish water) were to flow through a crude-oil layer that is susceptible to emulsion formation.

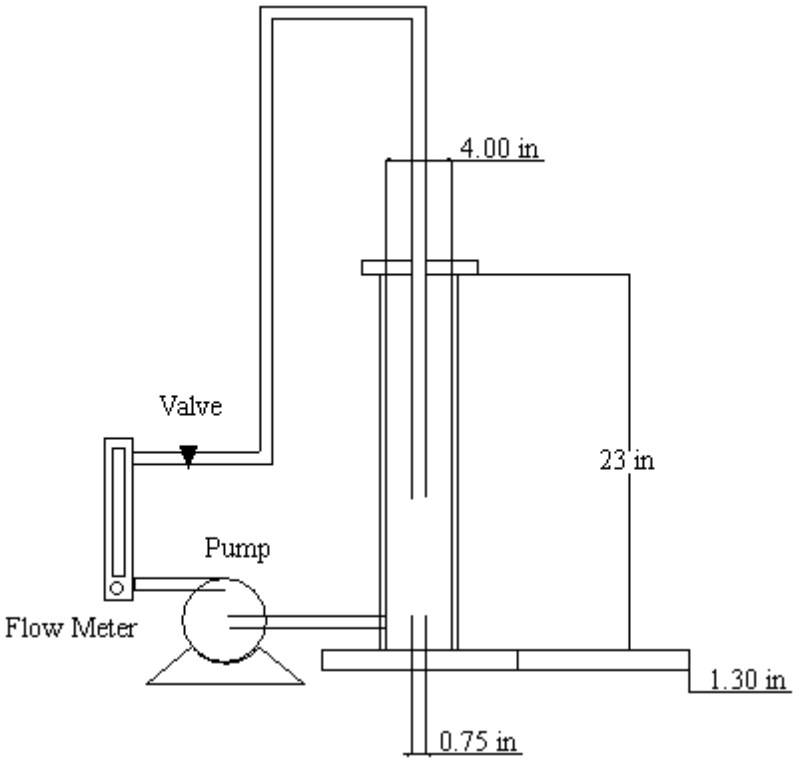

Figure 12. Schematic of the small-scale SPR tank setup.

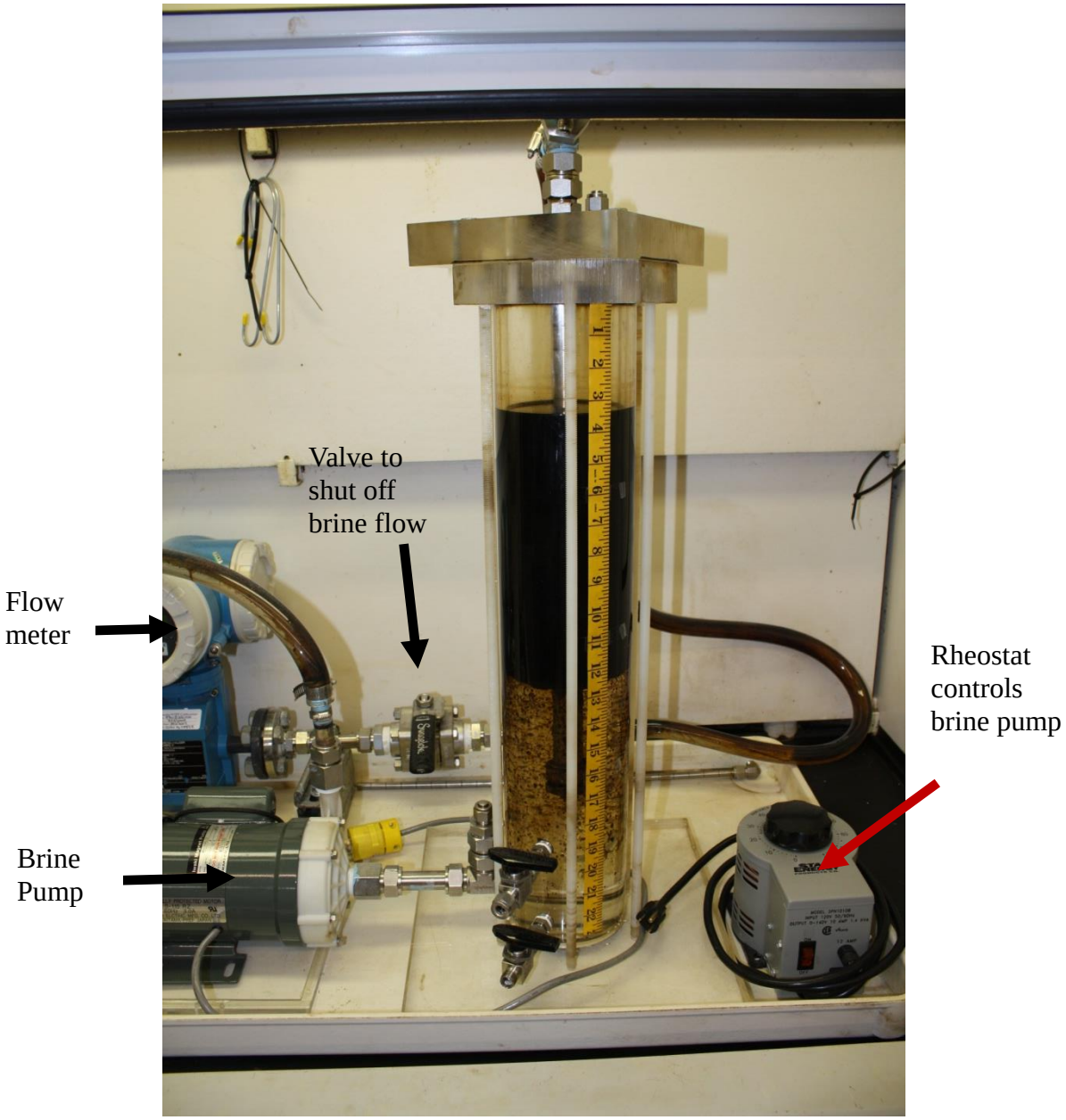

Figure 13. Image of small-scale-tank setup containing well-head-sampled Big Hill cavern 106 crude oil and 5 m NaCl. In the image the flow meter, valve, and pump are on the left and the rheostat is on the right.

7.1.1 Experimental Methodology

7.1.1.1 Parameterization of the problem

The parameters that have been varied in this experiment include: the velocity exiting the jet nozzle, and the jet-nozzle diameter. The dimensionless groups corresponding to these parameters are the jet Reynolds number,

$$\mathrm{Re}_{Jet} = \frac{\rho_b v d}{\mu_b}, \tag{1}$$

and the jet Weber number based on the jet diameter,

$$We_{Jet} = \frac{\rho_b v^2 d}{\sigma}. \tag{2}$$

Here ρ_b is the density of the brine phase (g/L), v is the velocity at the nozzle exit (m/sec), d is the nozzle diameter (m), μ_b is the viscosity of the brine phase (cP), σ is the oil-brine interfacial tension (N/m), and $a_{\max}$ is the largest stable drop size (m) in the stable brine-in-crude-oil emulsion (probably oil dependent). For the drop-scale Weber number we have assumed $a_{\max}$ ~ 100 µm, based on the drop-size distribution given in Figure 14. Figure 14 was obtained from analyzing a stable emulsion produced from a test using a 1/8 in nozzle and a flow rate of 2.1 gal/min (8 L/min). Drop diameters were measured using a confocal microscope (Olympus BX60), a calibrated reticule (Graticules LTD model SC 467), and the ImageJ image-analysis software. A small drop of emulsion was placed on a glass slide and imaged using the microscope without a coverslip or other disturbance.

Table 7 shows the parameter values used in calculating the dimensionless groups in equations (1) – (2). Table 8 shows the range of Re_{Jet} and We_{Jet}, explored in this experiment and SPR relevant values for comparison.

Table 7. Parameter values used in this report.

Sample	*Specific Gravity*[1] (dimensionless)	μ_b[2] (cP)	σ[3] (N/m)
5m NaCl	1.18	1.3	0.028
SPR Raw Intake water	1.00	1	0.028

1. Based on measurements of 5 m NaCl and Bryan Mound raw water using a pipette, deionized water at 72-77 °F (22-25 °C) and a high-precision balance.

2. Based on viscosity measurements of 5 m NaCl and BM raw water using a Fann viscometer (accurate to 1 – 2 significant figures).

3. Based on data from NMT between BH raw water and BH cavern 106 crude oil, see Table 5 in Appendix B.

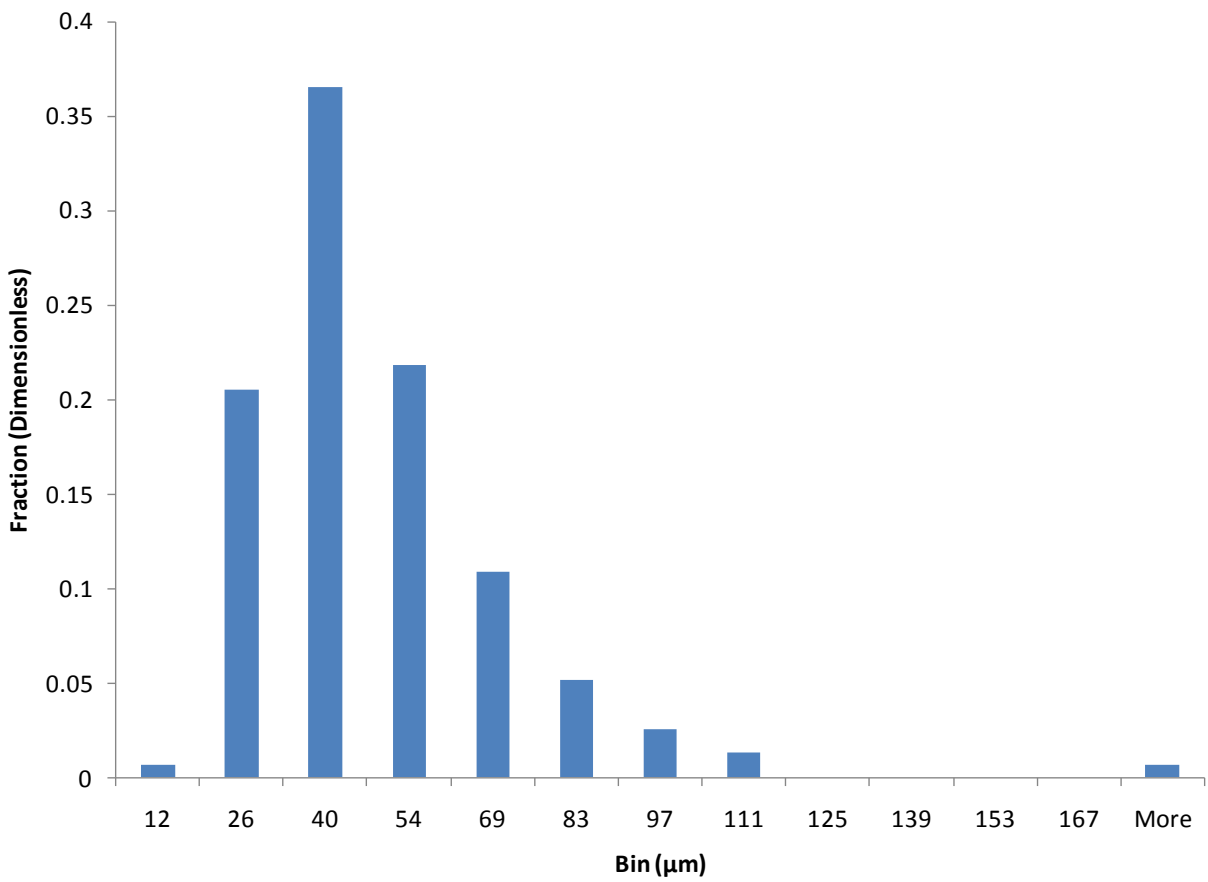

Figure 14. Drop-size (diameter) distribution for a stable emulsion obtained from the 1/8 in jet-nozzle test at a flow rate of 2.1 gal/min (8 L/min).

Table 8. Comparison of experimental flow parameters to those applicable to SPR.

	Velocity, *v* (m/sec or ft/sec)	Re_{Jet} (dimensionless)	We_{Jet} (dimensionless)
This report	0.92 – 55 ft/sec (0.3-17 m/sec)	2300-47,000	30-38,000
SPR[1]	11.7 ft/sec (3.6 m/sec)	10^6	10^5

1. Based on a drawdown of 95,000 bbl/day through a 9.85 in pipe.

7.1.1.2 Procedure

The experimental procedure is depicted in Figure 15 and was as follows:

1) Put a jet nozzle with known orifice diameter onto the brine string.

2) Record the at-rest oil-brine interface height from the tape measure affixed to the outside of the small-scale SPR tank.

3) Move the brine string such that the nozzle exit is located in the brine layer. Turn on the pump, set the flow rate to a desired value, Figure 15a.

4) Close brine valve, move the brine string up such that the jet nozzle exit is located at the top of the oil column, Figure 15b.

5) Begin recording video using JVC camera.

6) Open the brine valve to allow brine to flow into the crude oil layer. Record flow rate (liters/sec) from the flow meter, Figure 15c.

7) Close the brine valve when the black-brine-in-oil-mixture interface height reaches the bottom of the tank, specifically at 20 inches as read by the tape measure. Record total flow (liters) from flow meter, Figure 15d.

8) Continue recording video of the interface location versus time, Figure 15e-f.

For most nozzle diameters and flow rates, at least two runs were performed. An exception to this was when a stable emulsion was formed. We have explored velocities from 0.92 ft/sec (0.3 m/sec) up to 55 ft/sec (17 m/sec) and nozzle diameters from 1/8 in (3×10^{-3} m) up to 3/8 in (9×10^{-3} m).

For each run, 5 molal (m) NaCl brine (23 wt %) was used as the aqueous phase. Based on experience and the literature, we believe it is more difficult to form a stable emulsion with a nearly saturated brine than with brackish water (SPR raw water), because of the salting-out effect. Thus if we form a stable emulsion with 5 m NaCl at a given flow condition, we believe it is even more likely to happen for brackish or fresh water.

The crude oil used was from the well-head of Big Hill cavern 106. Jim Perry of DynMcDermott was gracious in sending us 16 liters of crude oil. As discussed in Subsection 4.2 of Nemer and Lord (2008), Big Hill cavern 106 oil has been found to form stable emulsions. All tests were performed at room temperature 72-77 °F (22-25 °C) and atmospheric pressure.

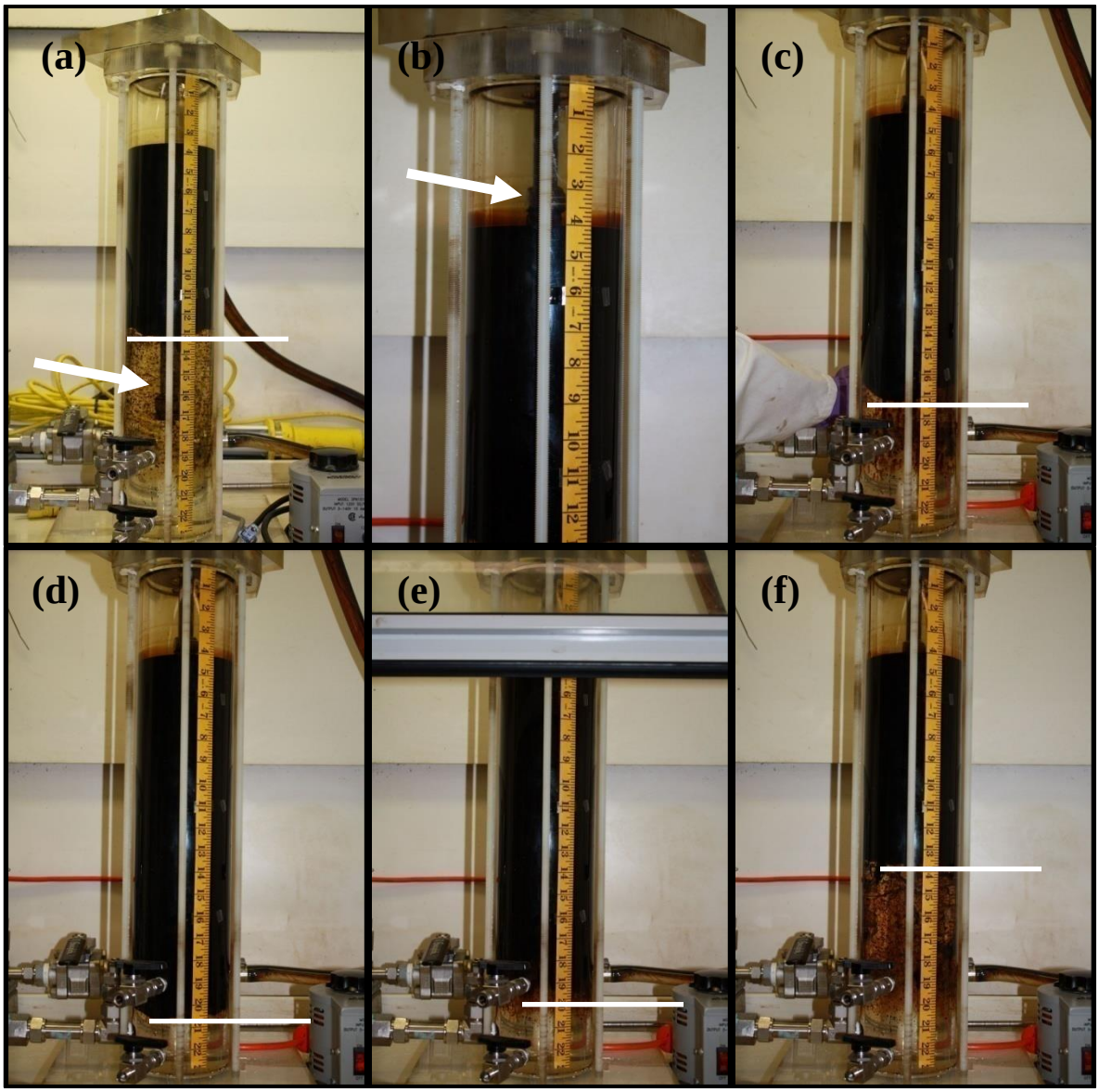

Figure 15. Sequence of steps in a SPR small-tank experiment: (a) place brine string (white arrow points to string, white line points to oil-brine interface) into the brine layer and set the flow rate to desired value; (b) close the brine valve, move brine string (arrow points to string) up such that the brine-jet orifice is at the top of the oil column; (c) open valve to allow brine to flow into the crude oil layer at the prescribed rate; (d) close valve when the black oil-brine mixture interface (white line) descends to a depth just above the inlet to the brine pump (20 inches on the tape measure); (e)-(f) record the interface height (white line) versus time as the emulsion breaks up into brine and crude oil.

7.1.2 Runs Performed

Table 9 contains a list of all runs performed to date using the small-scale SPR tank, BH 106 crude oil and 5 m NaCl brine. For each nozzle size a series of runs were performed in increasing flow rate. A photo of a stable brine-in-crude emulsion extracted from Run # 7 (Table 9) is shown in Figure 16.

Table 9. List of runs performed using the small-scale SPR tank. Note that Re and We are dimensionless.

Run Number	Jet Nozzle Diameter (in)	Flow Rate (gal/min)	Nozzle Velocity (ft/sec)	Re_{Jet}	We_{Jet}
1	0.125	0.1	3.6	3×10^3	2×10^2
2	0.125	0.3	6.9	6×10^3	6×10^2
3	0.125	0.3	6.9	6×10^3	6×10^2
4	0.125	0.3	6.9	6×10^3	6×10^2
5	0.125	0.3	6.9	6×10^3	6×10^2
6	0.125	0.8	21	2×10^4	6×10^3
7	0.125	2.1	55	5×10^4	4×10^4
8	0.25	1.1	6.9	1×10^4	1×10^3
9	0.25	1.1	7.4	1×10^4	1×10^3
10	0.25	2.1	14	2×10^4	5×10^3
11	0.25	2.2	14	2×10^4	5×10^3
12	0.25	2.6	17	3×10^4	7×10^3
13	0.375	0.3	0.92	2×10^3	3×10^1
14	0.375	0.4	1.1	3×10^3	5×10^1
15	0.375	0.4	1.3	3×10^3	6×10^1
16	0.375	0.5	1.4	3×10^3	7×10^1
17	0.375	0.5	1.6	4×10^3	9×10^1
18	0.375	1.0	2.9	7×10^3	3×10^2
19	0.375	1.0	3.0	8×10^3	3×10^2
20	0.375	1.1	3.1	8×10^3	3×10^2
21	0.375	1.1	3.2	8×10^3	4×10^2
22	0.375	2.1	6.2	2×10^4	1×10^3
23	0.375	2.1	6.2	2×10^4	1×10^3
24	0.375	2.1	6.2	2×10^4	1×10^3
25	0.375	4.2	12	3×10^4	6×10^3

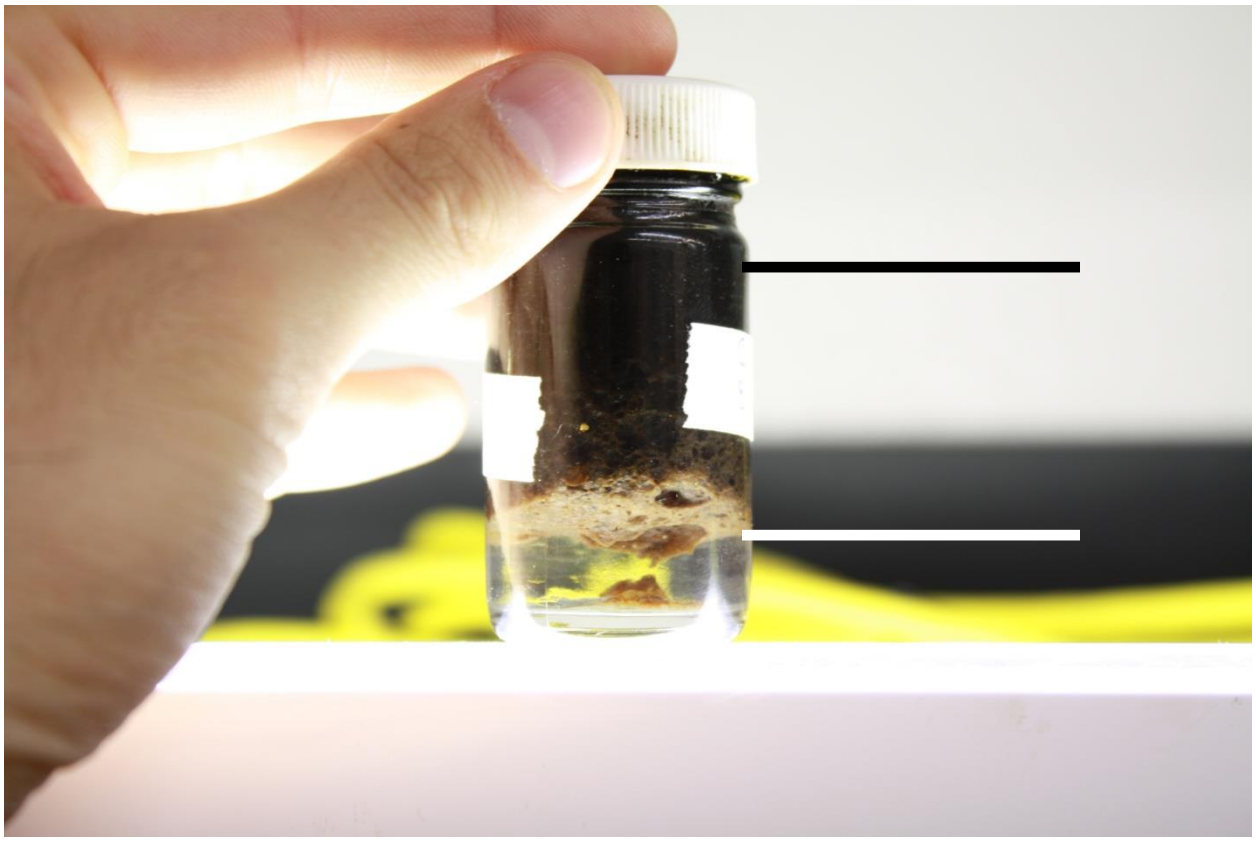

Figure 16. Image of stable-brine-in-crude-oil emulsion obtained from the 1/8 inch jet nozzle at a flow rate of 2.1 gal/min (8 L/min). The lower fluid is brine that has separated. Oil has also separated on top of the emulsion. The white line marks the emulsion-brine interface, and the black line approximately marks the oil-emulsion interface.

7.1.3 Results

The main result of the work in the small-scale SPR tank is that for any operationally relevant flow rate ($Re_{Jet} > 10^3$) of brine into the crude-oil layer, brine does not flow straight through the crude-oil layer into the brine layer but instead becomes entrained as an emulsion in the crude oil which takes time to separate, if it separates at all (see Figure 15c-d). This result is shown quantitatively in Figure 17, which plots the fraction of brine entrained in the crude oil once the pump is turned off. At $Re_{Jet} \sim 10^4$, all of the brine that has been flowed into the crude oil has been held up, temporarily for un-stable emulsions and permanently for stable emulsions.

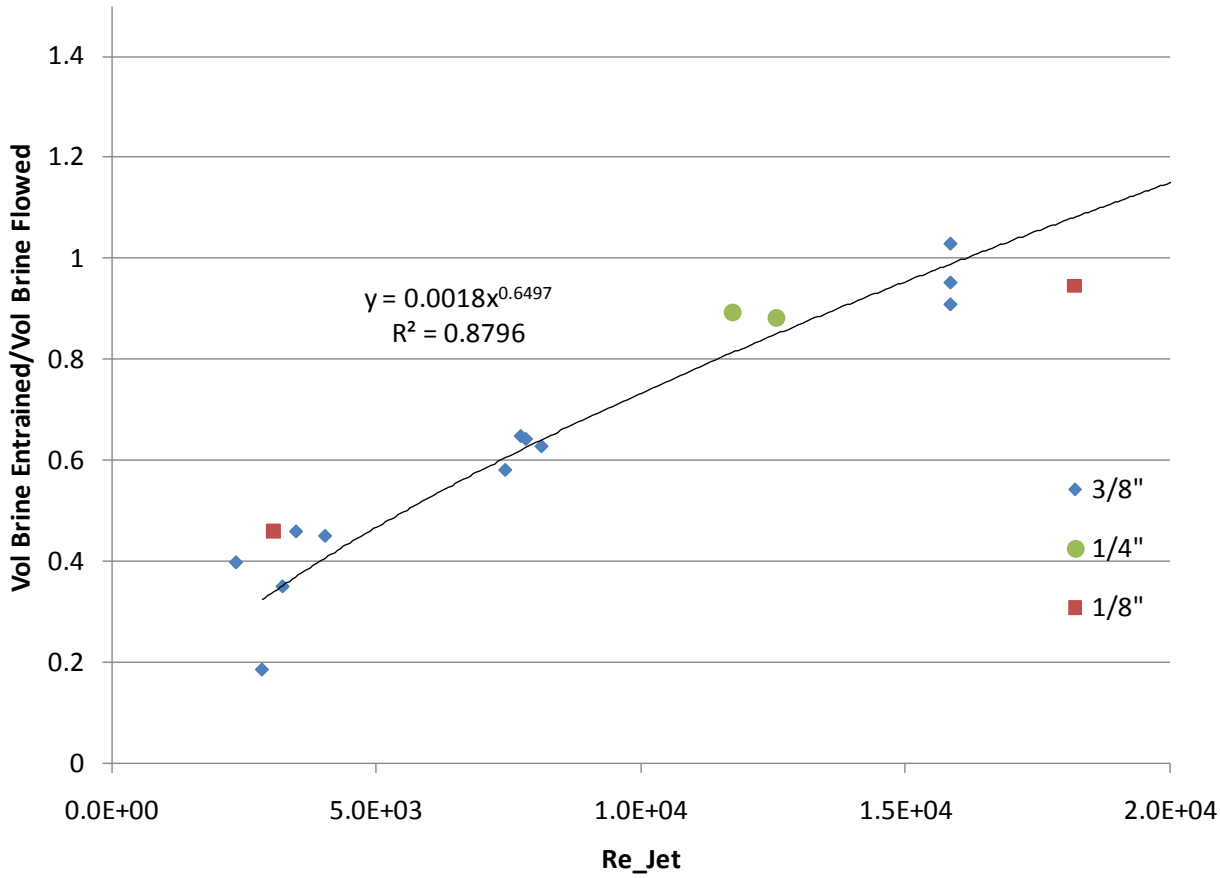

Figure 17. Fraction of brine that becomes entrained in the crude oil during flow of brine into the crude oil. The different symbols correspond to different nozzle sizes: 1/8 in, 1/4 in, and 3/8 in. See Table 8 for scaling to SPR conditions.

7.2 Recovery Times and Stable Emulsion Formation

The recovery time is the amount of time required for the unstable black-brine-in-oil interface to return to its original height (before the flow test was begun) determined from the recorded video, as a function of the flow conditions used to prepare that emulsion. A limitation of this observational method is that we can only approach flow rates that produce a stable emulsion, since the recovery time becomes meaningless when a permanent brine-in-crude-oil emulsion is produced. Figure 18 shows the recovery time normalized by the amount of time that the brine pump was on versus the jet-scale Reynolds number. Figure 18 shows the recovery time in minutes versus Re_{Jet}. It is clear that the time required for the emulsion to break increases with increasing Re_{Jet}.

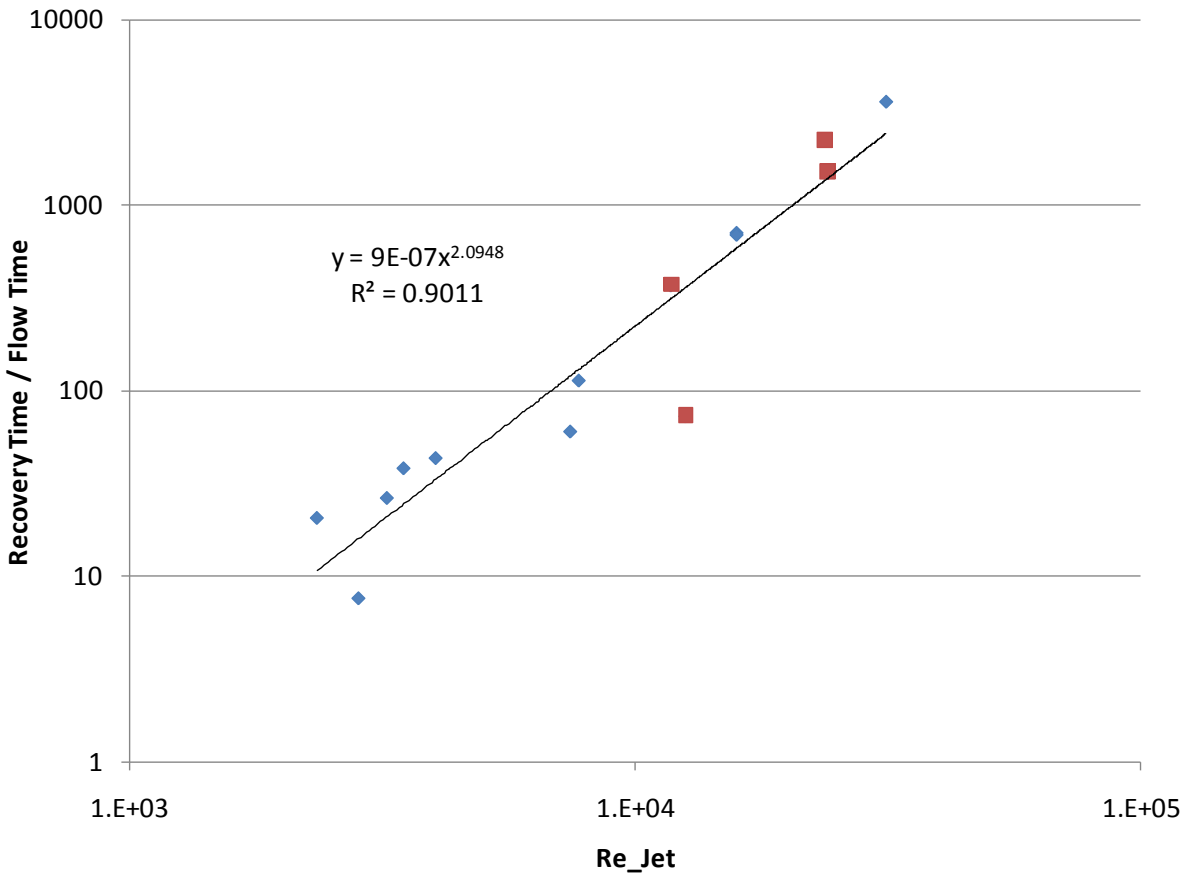

Figure 18. Time required for the unstable black-brine-in-oil interface to return to its original height (before the flow test was begun) normalized by the time during which brine was pumped through the oil layer, versus the jet Reynolds number, Re_{Jet} (dimensionless).

8 BOTTLE TESTS ON ALL SPR OILS

All of the SPR sites conducted bottle tests on downhole-sampled oil samples and raw-intake water to determine which cavern oils are susceptible to stable emulsion formation. The downhole oil samples used were previously collected under the existing DynMcDermott downhole sampling manual (U. S. Department of Energy, 2009) and are stored in refrigerated storage at Northrup Grumman Corp. Not all cavern oils were tested as DynMcDermott decided that some caverns have had too extensive oil movements (generally > 15 vol % since the downhole oil samples were collected) for the downhole samples to be relevant to current inventories.

For each bottle test, DynMcDermott reports the oil-water interface height versus time, and the interface height in the bottles before they are shaken. These heights were obtained from ruled markings affixed to the bottle. From this information we calculated

$$Vol_{water}\,\% = 100\frac{I_i - I_f}{I_i}\,, \tag{3}$$

where I_i is the initial oil-water interface height before the bottle is shaken, and I_f is the oil-water interface height after the bottle is shaken, measured at different times. The interface height is read from an external measuring tape affixed to the bottle. Equation (3) is interpreted to be the fraction of water that remains "held up" in the oil phase. This should not be confused with the volume fraction of water in the oil phase, as some oil will separate off the top of the emulsion just as some water separates off the bottom.

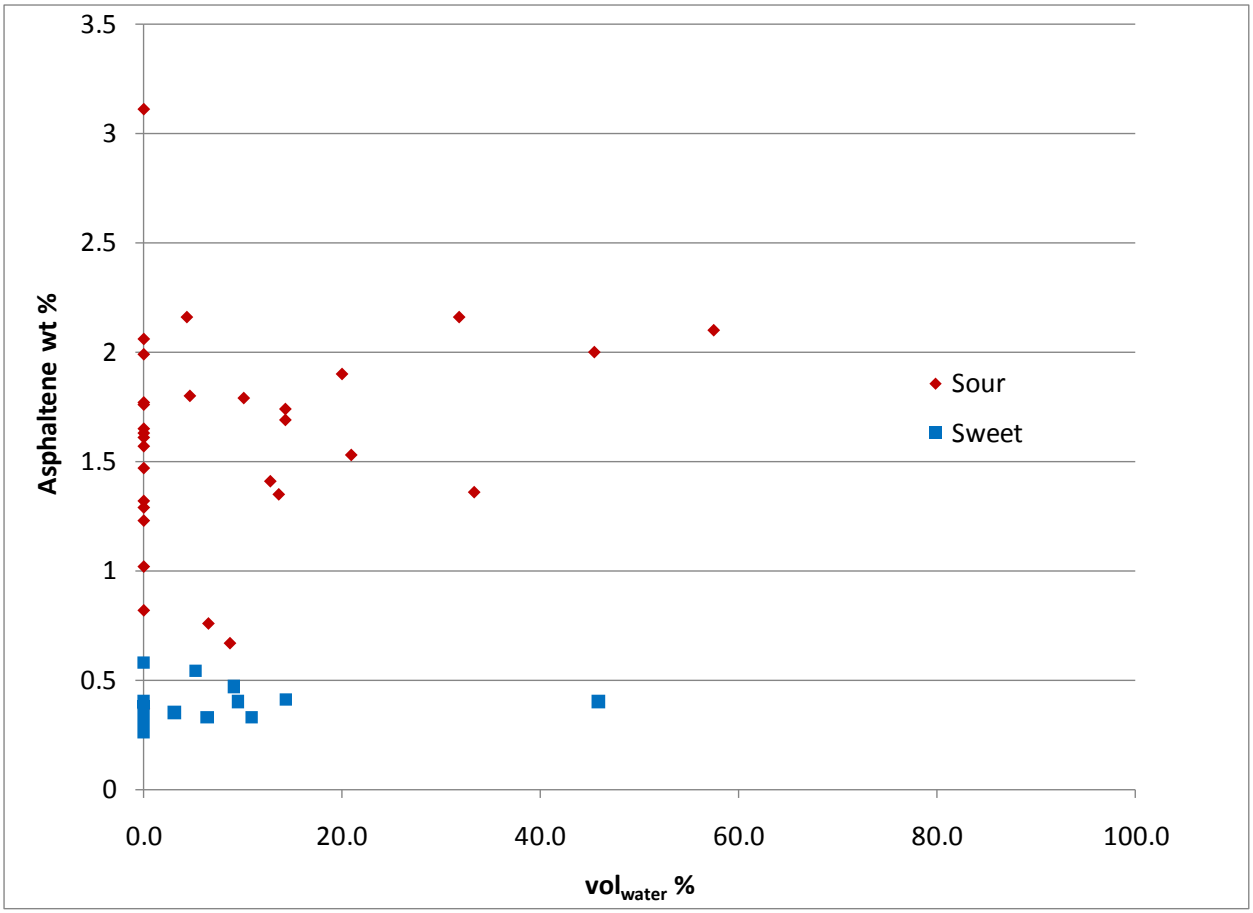

Figure 19. Asphaltene wt % versus vol_{water} %. Bottle tests on oils that do not have an asphaltene assay are not plotted.

For each of the results reported to us by DynMcDermott we calculated vol_{water} % using equation (3). A plot of asphaltene wt % versus vol_{water} % is shown in Figure 19. The vol_{water} % and asphaltene wt % for each cavern are also shown below in Table 10 approximately 3 months after the tests were begun; Table 11 gives a list of caverns that do not have a bottle test result. Figure 19 shows two populations: a sweet population at lower asphaltene wt %, and a sour population at higher asphaltene wt %. The majority of those samples with a vol_{water} % above 20 %, are sour and have a high asphaltene wt %. However there is an outlier, downhole-sampled BM002, which is a sweet cavern with a low asphaltene wt % and a high vol_{water} %. Bottle tests on oils that do not have an asphaltene assay are not plotted in Figure 19.

In Appendix B we have included the full table of bottle test results versus time. These results should be considered when examining drawdowns or delaying workovers on caverns with shortened/broken hanging strings. Many of the caverns show significant water hold up for the first several days. We caution the reader that the bottle tests were designed to gauge the stability of the emulsions, not the time dependent behavior of emulsion separation. Nonetheless, we believe that they may be a useful guide.

Table 10. Bottle test results for downhole-sampled SPR oils reported approximately 3 months after the tests were begun. Here we give vol_{water} %, asphaltene wt %, wax wt %, type of oil (sweet or sour) from SPR site bottle tests, and test duration, organized by site. The asphaltene and wax wt % were obtained from DynMcDermott oil quality data sheets.

Cavern ID	Vol_{water} %	Asphaltene wt %	Wax wt %	Sweet/Sour	Days since Shaken
BH101	10.9	0.33	0.05	Sweet	97
BH102	0.0	1.02	0.52	Sour	97
BH103	0.0	0.26	0.78	Sweet	97
BH104	3.0	0.35	0.07	Sweet	97
BH105	5.2	0.54	0.46	Sweet	97
BH106	57.5	2.1	0.06	Sour	97
BH107	45.5	2	0.41	Sour	97
BH108	20.0	1.9	0.18	Sour	97
BH109	20.9	1.53	0.06	Sour	97
BH110	0.0	1.76		Sour	97
BH111	0.0	1.57	0.09	Sour	97
BH112	10.1	1.79	0.24	Sour	97
BH113	0.0	1.77	0.26	Sour	97
BH114	0.0	0.37	0.38	Sour	97
BC101	33.3	1.36	0.05	Sour	98
BC17	4.7	1.8	0.08	Sour	98
BC18	0.0	0.38	1.1	Sweet	98
BC19	0.0	1.32	0.1	Sour	98
BC20	0.0	0.58		Sweet	98
BC15	0.0	0.82	0.21	Sour	98
WH006	12.8	1.41	0.16	Sour	94
WH007	0.0	0.23	0.12	Sweet	94
WH008	8.7	0.67		Sour	94
WH009	0.9	0.80	5.8	Sour	94
WH011	6.5	0.76		Sour	94
WH105	0.0	NA	NA	Sweet	94
WH106	14.3	1.74	0.06	Sour	94
WH108	6.4	0.33	0.26	Sweet	94
WH109	0.0	1.61	0.14	Sour	94
WH110	9.5	0.4	0.31	Sweet	94
WH111	0.0	1.29	0.26	Sour	94
WH112	13.6	1.35	0.18	Sour	94
WH114	0.0	1.23	0.68	Sour	94
WH115	0.0	1.47	0.15	Sour	94
WH116	0.8	NA	NA	Sweet	94

Cavern ID	Vol_{water} %	Asphaltene wt %	Wax wt %	Sweet/Sour	Days since Shaken
WH117	0.0	1.65	0.1	Sour	94
BM001	40.9	2.0		Sour	84
BM002	45.8	0.4	0.45	Sweet	84
BM004	13.0	0.29		Sweet	84
BM005	0.0	1.99	0.14	Sour	84
BM101	31.8	2.16	0.96	Sour	84
BM102	100.0	1.9		Sour	84
BM103	4.3	2.16		Sour	84
BM104	10.0	1.84		Sour	84
BM105	0.0	2.06		Sour	84
BM106	0.0	0.4		Sweet	84
BM107	14.3	1.69	0.22	Sour	84
BM108	35.0	2.1		Sour	84
BM109	0.0	1.34	0.49	Sour	84
BM110	0.0	3.11	0.14	Sour	84
BM111	0.0	1.63	0.7	Sour	84
BM113	0.0	0.32		Sweet	84
BM114	9.1	0.47	0.24	Sweet	84
BM115	14.3	0.41	0.17	Sweet	84
BM116	0.0	0.33	0.51	Sweet	84

Table 11. List of caverns that do not have a bottle test result. The refrigerated downhole samples for these caverns are no longer considered representative of current oil inventories.

Cavern ID
WH102
WH101
WH104
WH113
WH103
WH107
BM112

[This page intentionally blank]

9 CONCLUSIONS

We were not able to produce a theoretical description of stable brine-in-crude-oil emulsion formation in an SPR-like geometry as a function of flow conditions. However we believe that several pieces of useful information have been obtained. First, brine does not flow straight through the crude oil into the brine layer. It becomes entrained in the crude-oil layer and requires time to separate. Second, stable brine-in-crude-oil emulsions have been obtained in an SPR-like geometry at flow conditions that are far less vigorous than would be encountered in a real SPR cavern. Third, from the data obtained thus far it seems unlikely that a reasonable flow rate can be found that would prevent permanent emulsification in a real SPR cavern, if brine were to flow through a crude-oil layer that is susceptible to permanent emulsion formation. Fourth, stable emulsions have been found to loosely correlate with sour oils with a high asphaltene concentration. Fifth, water-based de-emulsifying compounds work well and deserve further consideration.

[This page intentionally blank]

REFERENCES

Barenblatt, G. I. *Scaling, self-similarity, and intermediate asymptotics*. Cambridge Texts in Applied Mathematics. edited by D. G. Crighton Cambridge, United Kingtom: Cambridge University Press, 1996.

Eley, D. D., M. J. Hey, and J. D. Symonds. "Emulsions of Water in Asphaltene-Containing Oils; 1. Droplet Size Distribution and Emulsification Rates." *Colloids and Surfaces* 32 (1988): 87-101.

Fan, Y., S. Simon, and J. Sjoblom. "Chemical Destabilization of Crude Oil Emulsions: Effect of Nonionic Surfactants as Emulsion Inhibitors." *Energy & Fuels* 23 (2009): 4575-83.

Fingas, M., and B. FieldHouse. "Studies of the formation process of water-in-oil emulsions." *Marine Pollution Bulletin* 47 (2003): 369-96.

Gafonova, O. V., and W. Yarranton. "The Stabilization of Water-in-Hydrocarbon Emulsions by Asphaltenes and Resins." *Journal of Colloid and Interface Science* 241 (2001): 469-78.

Goldszal, A., and M. Bourrel. "Demulsification of Crude Oil Emulsions: Correlations to Microemulsion Phase Behavior." *Ind. Eng. Chem. Res.* 39 (2000): 2746-51.

Kilpatrick, P. K. "Water-in-Crude Oil Emulsion Stabilization: Review and Unanswered Questions." *Energy & Fuels* 26, No. 7 (2012): 4017-26.

Lee, R. F. "Agents Which Promote and Stabilize Water-in-Oil Emulsions." *Spill Science & Technology Bulletin* 5, No. 2 (1999): 117-26.

McLean, J. D., and P. K. Kilpatrick. "Effects of Asphaltene Aggregation in model heptane-toluene mixtures on stability of water-in-oil emulsions." *Journal of Colloid and Interface Science* 196 (1997): 23-24.

Nemer, M., and D. Lord, *Emulsions from Raw Water Injection Through Broken Hanging String, March 31'st, 2008 Progress Report for Subtask 2.3*, Sandia National Laboratories, Carlsbad, NM 2008.

Pena, A. A., G. J. Hirasaki, and C. A. Miller. "Chemically Induced Destabilization of Water-in-Crude Oil Emulsions." *Ind. Eng. Chem. Res.* 44 (2005): 1139-49.

Poindexter, M. K., S. Chuai, R. A. Marble, and M. S. C. "Solid Content Dominates Emulsion Stability Predictions." *Energy and Fuels* 19 (2005): 1346-52.

Sjoblom, J., O. Urdahl, K. G. Nordli Borve, M. Li, J. O. Saeten, A. A. Christy, and T. Gu. "Stabilization and Destabilization of Water-in-Crude Oil Emulsions from the Norwegian Continental Shelf. Correlation with Model Systems.". *Advances in Colloid and Interface Science* 41 (1992): 241-71.

Spiecker, P. M., K. L. Gawrys, C. B. Trail, and P. K. Kilpatrick. "Effects of petroleum resins on asphaltene aggregation and water-in-oil emulsion formation." *Colloids and Surfaces A: Physiochem. Eng. Aspects* 220 (2003): 9-27.

Thompson, D. G., A. S. Taylor, and D. E. Graham. "Emulsification and Demulsification Related to Crude Oil Production." *Colloids and Surfaces* 15 (1985): 175-89.

U. S. Department of Energy, *Crude Oil Quality Program and Test Criteria*, SPRPMO O 413.1C Chg 1. Strategic Petroleum Reserve, New Orleans, LA 2004.

U. S. Department of Energy, *DOE Manual SPRPMO M 413.1-1A, Crude Oil Quality Program and Test Criteria Manual*, DOE, New Orleans, LA 2009.

APPENDIX A. COMPLETE OIL BLENDING EXPERIMENTAL DATA

Table 12. Raw data from the blended oil experiments.

Oil A			Oil B			Oil A + Oil B	Oil + Brine	Free Oil	Time Between Mixing and
Sample ID	Vol. (mL)	Asphaltene (wt %)	Sample ID	Vol (mL)	Asphaltene (wt %)	Asphaltene (wt %)	Visual Separation	(g)	Free Oil Weighing (Hrs.)
CAV106 A	3	3.1	CAV101A	12	1.2	1.58	Yes - Max Separation	11.76	330.5
CAV106 A	3.5	3.1	CAV101A	11.5	1.2	1.64	No	6.36	305.5
CAV106 A	4	3.1	CAV101A	11	1.2	1.71	No	9.14	307.25
CAV106 A	5	3.1	CAV101A	10	1.2	1.83	No	7.81	359
CAV106 A	5	3.1	CAV101A	10	1.2	1.83	No	7.48	358.5
CAV106 A	10	3.1	CAV101A	5	1.2	2.47	No	7.58	359.25
CAV106 A	10	3.1	CAV101A	5	1.2	2.47	No	7.23	359
CAV106 A	1	3.1	CAV105A	14	1.1	1.23			
CAV106 A	2	3.1	CAV105A	13	1.1	1.37			
CAV106 A	3	3.1	CAV105A	12	1.1	1.50	Yes - Min Separation	8.09	71
CAV106 A	4	3.1	CAV105A	11	1.1	1.63	Yes - Min Separation	7.96	70.5
CAV106 A	5	3.1	CAV105A	10	1.1	1.77	No	7.08	71.75
CAV106 A	6	3.1	CAV105A	9	1.1	1.90	No	7.56	71.75
CAV108A	1	3.1	CAV102A	14	1.7	1.79	Yes - Max Separation	12.14	21
CAV108A	2	3.1	CAV102A	13	1.7	1.89	Yes - Max Separation	10.73	20.25
CAV108A	3	3.1	CAV102A	12	1.7	1.98	Yes - Modest Separate	10.27	66

Oil A			Oil B			Oil A + Oil B	Oil + Brine	Free Oil	Time Between Mixing and
Sample ID	Vol. (mL)	Asphaltene (wt %)	Sample ID	Vol (mL)	Asphaltene (wt %)	Asphaltene (wt %)	Visual Separation	(g)	Free Oil Weighing (Hrs.)
CAV108A	4	3.1	CAV102A	11	1.7	2.07	Yes - Modest Separate	10.16	20
CAV108A	5	3.1	CAV102A	10	1.7	2.17	Yes - Modest Separate	10.2	17.5
CAV108A	6	3.1	CAV102A	9	1.7	2.26	Yes - Modest Separate	9.96	17.5
CAV108A	7	3.1	CAV102A	8	1.7	2.35	Yes- Modest Separate		
CAV108A	9	3.1	CAV102A	6	1.7	2.54	Yes- Minimum Separation		
CAV108A	4	3.1	CAV103A	11	0.9	1.49	Yes - Max Separation	10.7	72
CAV108A	4.5	3.1	CAV103A	10.5	0.9	1.56	Yes - Modest Separate	11.58	71
CAV108A	5	3.1	CAV103A	10	0.9	1.63	Yes - Modest Separate	10.25	71.75
CAV108A	5.5	3.1	CAV103A	9.5	0.9	1.71	Yes - Min Separation	10.3	66.5
CAV108A	6	3.1	CAV103A	9	0.9	1.78	Yes - Min Separation	10.42	66
CAV108A	7	3.1	CAV103A	8	0.9	1.93			
CAV108A	8	3.1	CAV103A	7	0.9	2.07			
CAV108A	9	3.1	CAV103A	6	0.9	2.22			
CAV108A	1	3.1	CAV105A	14	1.1	1.23			
CAV108A	2	3.1	CAV105A	13	1.1	1.37			

Oil A			Oil B			Oil A + Oil B	Oil + Brine	Free Oil	Time Between Mixing and
Sample ID	Vol. (mL)	Asphaltene (wt %)	Sample ID	Vol (mL)	Asphaltene (wt %)	Asphaltene (wt %)	Visual Separation	(g)	Free Oil Weighing (Hrs.)
CAV108A	3	3.1	CAV105A	12	1.1	1.50	Yes - Min Separation	8.29	72
CAV108A	4	3.1	CAV105A	11	1.1	1.63	Yes - Min Separation	7.82	71.75
CAV108A	5	3.1	CAV105A	10	1.1	1.77	Yes - Min Separation	7.91	71.25
CAV108A	6	3.1	CAV105A	9	1.1	1.90	No	7.72	71.25
CAV111A	6	2.4	CAV103A	9	0.9	1.50	Yes - Min Separation	12.59	68
CAV111A	8	2.4	CAV103A	7	0.9	1.70	No	9.56	19.75
CAV111A	9	2.4	CAV103A	6	0.9	1.80	No	8.49	19.5
CAV111A	10	2.4	CAV103A	5	0.9	1.90	No	9.37	19.5

APPENDIX B: FULL DOWNHOLE-SAMPLED CRUDE OIL BOTTLE TEST RESULTS WITH TIME

Shown below are the bottle test results for all SPR downhole-sampled oils tested. The date column refers to the date a measurement was made, elapsed time is the time (days) from when the bottle was shaken, cavern id is self-explanatory, and vol_{water} % is given by Equation (3).

Date	Elapsed Time (days)	Cavern ID	Vol_{water} %
5/25/2010	0	BC15	100
5/27/2010	2	BC15	7
6/3/2010	9	BC15	2
6/7/2010	13	BC15	0
8/4/2010	71	BC15	0
8/30/2010	97	BC15	0
5/24/2010	0	BC17	100
5/25/2010	1	BC 17	37
5/27/2010	3	BC17	19
6/3/2010	10	BC17	16
6/7/2010	14	BC17	12
8/4/2010	72	BC17	9
8/30/2010	98	BC 17	5
5/24/2010	0	BC18	2
5/25/2010	1	BC18	0
5/27/2010	3	BC18	0
6/1/2010	8	BC18	0
6/2/2010	9	BC18	0
6/3/2010	10	BC18	0
6/7/2010	14	BC18	0
8/4/2010	72	BC18	0
8/30/2010	98	BC18	0
5/24/2010	0	BC19	2
5/25/2010	1	BC19	0
5/27/2010	3	BC19	0
6/1/2010	8	BC19	0
6/2/2010	9	BC19	0
6/3/2010	10	BC19	0
6/7/2010	14	BC19	0
8/4/2010	72	BC19	0
8/30/2010	98	BC19	0
5/24/2010	0	BC20	4
5/25/2010	1	BC20	0
5/27/2010	3	BC20	0

Date	Elapsed Time (days)	Cavern ID	Vol_{water} %
6/1/2010	8	BC20	0
6/2/2010	9	BC20	0
6/3/2010	10	BC20	0
6/7/2010	14	BC20	0
8/4/2010	72	BC20	0
8/30/2010	98	BC20	0
5/24/2010	0	BC101	100
5/25/2010	1	BC101	100
5/27/2010	3	BC101	100
6/1/2010	8	BC101	81
6/2/2010	9	BC101	57
6/3/2010	10	BC101	52
6/7/2010	14	BC101	48
8/4/2010	72	BC101	38
8/30/2010	98	BC101	33
5/25/2010	0	BH101	17
5/25/2010	0	BH101	2
5/27/2010	2	BH101	9
6/1/2010	7	BH101	11
6/2/2010	8	BH101	11
6/7/2010	13	BH101	9
8/2/2010	69	BH101	13
8/30/2010	97	BH101	11
5/25/2010	0	BH102	100
5/26/2010	1	BH102	5
5/27/2010	2	BH102	14
6/1/2010	7	BH102	0
6/2/2010	8	BH102	1
6/7/2010	13	BH102	0
8/2/2010	69	BH102	1
8/30/2010	97	BH102	0
5/25/2010	0	BH103	15
5/26/2010	1	BH103	2
5/27/2010	2	BH103	1
6/1/2010	7	BH103	2
6/2/2010	8	BH103	1
6/7/2010	13	BH103	1
8/2/2010	69	BH103	2
8/30/2010	97	BH103	0
5/25/2010	0	BH104	9
5/26/2010	1	BH104	3

Date	Elapsed Time (days)	Cavern ID	Vol_{water} %
5/27/2010	2	BH104	3
6/1/2010	7	BH104	3
6/2/2010	8	BH104	0
6/7/2010	13	BH104	3
8/2/2010	69	BH104	7
8/30/2010	97	BH104	3
5/25/2010	0	BH105	13
5/26/2010	1	BH105	7
5/27/2010	2	BH105	7
6/1/2010	7	BH105	5
6/2/2010	8	BH105	2
6/7/2010	13	BH105	2
8/2/2010	69	BH105	5
8/30/2010	97	BH105	5
5/25/2010	0	BH106	100
5/26/2010	1	BH106	100
5/27/2010	2	BH106	100
6/1/2010	7	BH106	36
6/2/2010	8	BH106	65
6/7/2010	13	BH106	60
8/2/2010	69	BH106	58
8/30/2010	97	BH106	58
5/25/2010	0	BH107	100
5/26/2010	1	BH107	100
5/27/2010	2	BH107	100
6/1/2010	7	BH107	100
6/2/2010	8	BH107	100
6/7/2010	13	BH107	68
8/2/2010	69	BH107	49
8/30/2010	97	BH107	45
5/25/2010	0	BH108	100
5/26/2010	1	BH108	69
5/27/2010	2	BH108	62
6/1/2010	7	BH108	36
6/2/2010	8	BH108	40
6/7/2010	13	BH108	49
8/2/2010	69	BH108	34
8/30/2010	97	BH108	20
5/25/2010	0	BH109	100
5/26/2010	1	BH109	72
5/27/2010	2	BH109	70

Date	Elapsed Time (days)	Cavern ID	Vol_{water} %
6/1/2010	7	BH109	44
6/2/2010	8	BH109	37
6/7/2010	13	BH109	33
8/2/2010	69	BH109	23
8/30/2010	97	BH109	21
5/25/2010	0	BH110	0
5/26/2010	1	BH110	0
5/27/2010	2	BH110	0
6/1/2010	7	BH110	0
6/2/2010	8	BH110	0
6/7/2010	13	BH110	0
8/2/2010	69	BH110	0
8/30/2010	97	BH110	0
5/25/2010	0	BH111	100
5/26/2010	1	BH111	36
5/27/2010	2	BH111	20
6/1/2010	7	BH111	8
6/2/2010	8	BH111	3
6/7/2010	13	BH111	0
8/2/2010	69	BH111	0
8/30/2010	97	BH111	0
5/25/2010	0	BH112	100
5/26/2010	1	BH112	63
5/27/2010	2	BH112	46
6/1/2010	7	BH112	23
6/2/2010	8	BH112	22
6/7/2010	13	BH112	18
8/2/2010	69	BH112	10
8/30/2010	97	BH112	10
5/25/2010	0	BH113	100
5/26/2010	1	BH113	69
5/27/2010	2	BH113	54
6/1/2010	7	BH113	18
6/2/2010	8	BH113	15
6/7/2010	13	BH113	13
8/2/2010	69	BH113	0
8/30/2010	97	BH113	0
5/25/2010	0	BH114	23
5/26/2010	1	BH114	2
5/27/2010	2	BH114	6
6/1/2010	7	BH114	0

Date	Elapsed Time (days)	Cavern ID	Vol_{water} %
6/2/2010	8	BH114	0
6/7/2010	13	BH114	0
8/2/2010	69	BH114	0
8/30/2010	97	BH114	0
8/9/2010	0	BM001	100
8/10/2010	1	BM001	77
8/11/2010	2	BM001	77
8/12/2010	3	BM001	68
8/16/2010	7	BM001	68
8/17/2010	8	BM001	64
8/18/2010	9	BM001	64
8/19/2010	10	BM001	64
9/15/2010	37	BM001	55
10/6/2010	58	BM001	41
11/1/2010	84	BM001	41
12/1/2010	114	BM001	36
1/6/2011	150	BM001	36
8/9/2010	0	BM002	100
8/10/2010	1	BM002	67
8/11/2010	2	BM002	67
8/12/2010	3	BM002	58
8/16/2010	7	BM002	50
8/17/2010	8	BM002	50
8/18/2010	9	BM002	46
8/19/2010	10	BM002	46
9/15/2010	37	BM002	46
10/6/2010	58	BM002	46
11/1/2010	84	BM002	46
12/1/2010	114	BM002	42
1/6/2011	150	BM002	42
8/9/2010	0	BM004	100
8/10/2010	1	BM004	78
8/11/2010	2	BM004	70
8/12/2010	3	BM004	70
8/16/2010	7	BM004	65
8/17/2010	8	BM004	57
8/18/2010	9	BM004	57
8/19/2010	10	BM004	57
9/15/2010	37	BM004	57
10/6/2010	58	BM004	48
11/1/2010	84	BM004	13

Date	Elapsed Time (days)	Cavern ID	Vol_{water} %
12/1/2010	114	BM004	4
1/6/2011	150	BM004	4
8/9/2010	0	BM005	100
8/10/2010	1	BM005	100
8/11/2010	2	BM005	85
8/12/2010	3	BM005	85
8/16/2010	7	BM005	75
8/17/2010	8	BM005	65
8/18/2010	9	BM005	60
8/19/2010	10	BM005	60
9/15/2010	37	BM005	60
10/6/2010	58	BM005	25
11/1/2010	84	BM005	0
12/1/2010	114	BM005	0
1/6/2011	150	BM005	0
8/9/2010	0	BM101	100
8/10/2010	1	BM101	77
8/11/2010	2	BM101	55
8/12/2010	3	BM101	50
8/16/2010	7	BM101	41
8/17/2010	8	BM101	41
8/18/2010	9	BM101	36
8/19/2010	10	BM101	36
9/15/2010	37	BM101	32
10/6/2010	58	BM101	27
11/1/2010	84	BM101	32
12/1/2010	114	BM101	27
1/6/2011	150	BM101	27
8/9/2010	0	BM102	100
8/10/2010	1	BM102	100
8/11/2010	2	BM102	100
8/12/2010	3	BM102	100
8/16/2010	7	BM102	100
8/17/2010	8	BM102	100
8/18/2010	9	BM102	100
8/19/2010	10	BM102	100
9/15/2010	37	BM102	100
10/6/2010	58	BM102	100
11/1/2010	84	BM102	100
12/1/2010	114	BM102	100
1/6/2011	150	BM102	100

Date	Elapsed Time (days)	Cavern ID	Vol_{water} %
8/9/2010	0	BM103	100
8/10/2010	1	BM103	100
8/11/2010	2	BM103	100
8/12/2010	3	BM103	100
8/16/2010	7	BM103	100
8/17/2010	8	BM103	100
8/18/2010	9	BM103	100
8/19/2010	10	BM103	100
9/15/2010	37	BM103	100
10/6/2010	58	BM103	43
11/1/2010	84	BM103	4
12/1/2010	114	BM103	4
1/6/2011	150	BM103	4
8/9/2010	0	BM104	100
8/10/2010	1	BM104	60
8/11/2010	2	BM104	40
8/12/2010	3	BM104	30
8/16/2010	7	BM104	20
8/17/2010	8	BM104	15
8/18/2010	9	BM104	10
8/19/2010	10	BM104	10
9/15/2010	37	BM104	10
10/6/2010	58	BM104	10
11/1/2010	84	BM104	10
12/1/2010	114	BM104	10
1/6/2011	150	BM104	10
8/9/2010	0	BM105	100
8/10/2010	1	BM105	100
8/11/2010	2	BM105	100
8/12/2010	3	BM105	75
8/16/2010	7	BM105	65
8/17/2010	8	BM105	65
8/18/2010	9	BM105	65
8/19/2010	10	BM105	65
9/15/2010	37	BM105	35
10/6/2010	58	BM105	5
11/1/2010	84	BM105	0
12/1/2010	114	BM105	0
1/6/2011	150	BM105	0
8/9/2010	0	BM106	100
8/10/2010	1	BM106	0

Date	Elapsed Time (days)	Cavern ID	Vol_{water} %
8/11/2010	2	BM106	0
8/12/2010	3	BM106	0
8/16/2010	7	BM106	0
8/17/2010	8	BM106	0
8/18/2010	9	BM106	0
8/19/2010	10	BM106	0
9/15/2010	37	BM106	0
10/6/2010	58	BM106	0
11/1/2010	84	BM106	0
12/1/2010	114	BM106	0
1/6/2011	150	BM106	0
8/9/2010	0	BM107	100
8/10/2010	1	BM107	100
8/11/2010	2	BM107	100
8/12/2010	3	BM107	100
8/16/2010	7	BM107	100
8/17/2010	8	BM107	100
8/19/2010	10	BM107	100
9/15/2010	37	BM107	100
10/6/2010	58	BM107	29
11/1/2010	84	BM107	14
12/1/2010	114	BM107	10
1/6/2011	150	BM107	5
8/9/2010	0	BM108	100
8/10/2010	1	BM108	100
8/11/2010	2	BM108	100
8/12/2010	3	BM108	100
8/16/2010	7	BM108	100
8/17/2010	8	BM108	100
8/19/2010	10	BM108	100
9/15/2010	37	BM108	100
10/6/2010	58	BM108	75
11/1/2010	84	BM108	35
12/1/2010	114	BM108	35
1/6/2011	150	BM108	25
8/9/2010	0	BM109	100
8/10/2010	1	BM109	5
8/11/2010	2	BM109	0
8/12/2010	3	BM109	0
8/16/2010	7	BM109	0
8/17/2010	8	BM109	0

Date	Elapsed Time (days)	Cavern ID	Vol_{water} %
8/19/2010	10	BM109	0
9/15/2010	37	BM109	0
10/6/2010	58	BM109	0
11/1/2010	84	BM109	0
12/1/2010	114	BM109	0
1/6/2011	150	BM109	0
8/9/2010	0	BM110	100
8/10/2010	1	BM110	100
8/11/2010	2	BM110	100
8/12/2010	3	BM110	100
8/16/2010	7	BM110	100
8/17/2010	8	BM110	100
8/19/2010	10	BM110	100
9/15/2010	37	BM110	100
10/6/2010	58	BM110	10
11/1/2010	84	BM110	0
12/1/2010	114	BM110	0
1/6/2011	150	BM110	0
8/9/2010	0	BM111	100
8/10/2010	1	BM111	100
8/11/2010	2	BM111	100
8/12/2010	3	BM111	100
8/16/2010	7	BM111	100
8/17/2010	8	BM111	100
8/19/2010	10	BM111	100
9/15/2010	37	BM111	100
10/6/2010	58	BM111	11
11/1/2010	84	BM111	0
12/1/2010	114	BM111	0
1/6/2011	150	BM111	0
8/9/2010	0	BM113	100
8/10/2010	1	BM113	32
8/11/2010	2	BM113	32
8/12/2010	3	BM113	26
8/16/2010	7	BM113	21
8/17/2010	8	BM113	16
8/18/2010	9	BM113	16
8/19/2010	10	BM113	16
9/15/2010	37	BM113	0
10/6/2010	58	BM113	0
11/1/2010	84	BM113	0

Date	Elapsed Time (days)	Cavern ID	Vol_{water} %
12/1/2010	114	BM113	0
1/6/2011	150	BM113	0
8/9/2010	0	BM114	100
8/10/2010	1	BM114	100
8/11/2010	2	BM114	100
8/12/2010	3	BM114	100
8/16/2010	7	BM114	100
8/17/2010	8	BM114	100
8/19/2010	10	BM114	100
9/15/2010	37	BM114	100
10/6/2010	58	BM114	32
11/1/2010	84	BM114	9
12/1/2010	114	BM114	9
1/6/2011	150	BM114	9
8/9/2010	0	BM115	100
8/10/2010	1	BM115	100
8/11/2010	2	BM115	76
8/12/2010	3	BM115	62
8/16/2010	7	BM115	62
8/17/2010	8	BM115	62
8/19/2010	10	BM115	62
9/15/2010	37	BM115	52
10/6/2010	58	BM115	43
11/1/2010	84	BM115	14
12/1/2010	114	BM115	10
1/6/2011	150	BM115	5
8/9/2010	0	BM116	32
8/10/2010	1	BM116	0
8/11/2010	2	BM116	0
8/12/2010	3	BM116	0
8/16/2010	7	BM116	0
8/17/2010	8	BM116	0
8/18/2010	9	BM116	0
8/19/2010	10	BM116	0
9/15/2010	37	BM116	0
10/6/2010	58	BM116	0
11/1/2010	84	BM116	0
12/1/2010	114	BM116	0
1/6/2011	150	BM116	0
5/24/2010	0	WH006	100
5/25/2010	1	WH006	38

Date	Elapsed Time (days)	Cavern ID	Vol_{water} %
5/26/2010	2	WH006	26
5/27/2010	3	WH006	26
6/1/2010	8	WH006	6
6/2/2010	9	WH006	9
6/3/2010	10	WH006	6
6/29/2010	36	WH006	15
8/26/2010	94	WH006	13
5/24/2010	0	WH007	2
5/25/2010	1	WH007	0
5/26/2010	2	WH007	0
5/27/2010	3	WH007	0
6/1/2010	8	WH007	0
6/2/2010	9	WH007	0
6/3/2010	10	WH007	0
6/29/2010	36	WH007	0
8/26/2010	94	WH007	0
5/24/2010	0	WH008	100
5/25/2010	1	WH008	61
5/26/2010	2	WH008	52
5/27/2010	3	WH008	51
6/1/2010	8	WH008	20
6/2/2010	9	WH008	24
6/3/2010	10	WH008	20
7/29/2010	66	WH008	9
8/26/2010	94	WH008	9
5/24/2010	0	WH009	100
5/25/2010	1	WH009	32
5/26/2010	2	WH009	21
5/27/2010	3	WH009	13
6/1/2010	8	WH009	11
6/2/2010	9	WH009	0
6/3/2010	10	WH009	0
7/29/2010	66	WH009	2
8/26/2010	94	WH009	1
5/24/2010	0	WH011	100
5/25/2010	1	WH011	13
5/26/2010	2	WH011	9
5/27/2010	3	WH011	15
6/1/2010	8	WH011	4
6/2/2010	9	WH011	2
6/3/2010	10	WH011	2

Date	Elapsed Time (days)	Cavern ID	Vol_{water} %
6/29/2010	36	WH011	7
8/26/2010	94	WH011	7
5/24/2010	0	WH105	0
5/25/2010	1	WH105	0
5/26/2010	2	WH105	0
5/27/2010	3	WH105	0
6/1/2010	8	WH105	0
6/2/2010	9	WH105	0
6/3/2010	10	WH105	0
6/29/2010	36	WH105	0
8/26/2010	94	WH105	0
5/24/2010	0	WH106	100
5/25/2010	1	WH106	76
5/26/2010	2	WH106	67
5/27/2010	3	WH106	61
6/1/2010	8	WH106	14
6/2/2010	9	WH106	14
6/3/2010	10	WH106	14
7/29/2010	66	WH106	14
8/26/2010	94	WH106	14
5/24/2010	0	WH108	100
5/25/2010	1	WH108	36
5/26/2010	2	WH108	51
5/27/2010	3	WH108	30
6/1/2010	8	WH108	5
6/2/2010	9	WH108	4
6/3/2010	10	WH108	4
7/29/2010	66	WH108	6
8/26/2010	94	WH108	6
5/24/2010	0	WH109	4
5/25/2010	1	WH109	0
5/26/2010	2	WH109	0
5/27/2010	3	WH109	1
6/1/2010	8	WH109	0
6/2/2010	9	WH109	0
6/3/2010	10	WH109	0
7/29/2010	66	WH109	1
8/26/2010	94	WH109	0
5/24/2010	0	WH110	100
5/25/2010	1	WH110	1
5/26/2010	2	WH110	0

Date	Elapsed Time (days)	Cavern ID	Vol_{water} %
5/27/2010	3	WH110	3
6/1/2010	8	WH110	1
6/2/2010	9	WH110	1
6/3/2010	10	WH110	1
7/29/2010	66	WH110	12
8/26/2010	94	WH110	9
5/24/2010	0	WH111	100
5/25/2010	1	WH111	9
5/26/2010	2	WH111	16
5/27/2010	3	WH111	15
6/1/2010	8	WH111	3
6/2/2010	9	WH111	2
6/3/2010	10	WH111	3
7/29/2010	66	WH111	0
8/26/2010	94	WH111	0
5/24/2010	0	WH112	100
5/25/2010	1	WH112	57
5/26/2010	2	WH112	49
5/27/2010	3	WH112	43
6/1/2010	8	WH112	19
6/2/2010	9	WH112	15
6/3/2010	10	WH112	19
7/29/2010	66	WH112	16
8/26/2010	94	WH112	14
5/24/2010	0	WH114	2
5/25/2010	1	WH114	0
5/26/2010	2	WH114	0
5/27/2010	3	WH114	0
6/1/2010	8	WH114	0
6/2/2010	9	WH114	0
6/3/2010	10	WH114	0
7/29/2010	66	WH114	0
8/26/2010	94	WH114	0
5/24/2010	0	WH115	4
5/25/2010	1	WH115	0
5/26/2010	2	WH115	0
5/27/2010	3	WH115	0
6/1/2010	8	WH115	0
6/2/2010	9	WH115	0
6/3/2010	10	WH115	0
7/29/2010	66	WH115	0

Date	Elapsed Time (days)	Cavern ID	Vol_{water} %
8/26/2010	94	WH115	0
5/24/2010	0	WH116	6
5/25/2010	1	WH116	2
5/26/2010	2	WH116	2
5/27/2010	3	WH116	4
6/1/2010	8	WH116	2
6/2/2010	9	WH116	2
6/3/2010	10	WH116	1
7/29/2010	66	WH116	1
8/26/2010	94	WH116	1
5/24/2010	0	WH117	100
5/25/2010	1	WH117	8
5/26/2010	2	WH117	6
5/27/2010	3	WH117	8
6/1/2010	8	WH117	0
6/2/2010	9	WH117	0
6/3/2010	10	WH117	0
7/29/2010	66	WH117	1
8/26/2010	94	WH117	0

APPENDIX C: NEW MEXICO TECH REPORT

Properties of Sandia Oil Samples

Tianguang Fan and Jill Buckley
NM Petroleum Recovery Research Center
New Mexico Tech
5 October 2007

SAMPLES

Ten crude oil samples and eleven water samples were received for testing from Sandia on August 24, 2007. Each sample consisted of approximately 1 liter of fluid in a clear glass bottle with screw-on cap. Identifying information from the labels is summarized in Table 1.

Table 1. Identification of Oil and Water Samples

Oil	from	ID #	Bottle #	Type
101	C101	BH070822-001	5232	swt
102	C102	BH070822-005	5236	swt
103	Cav 103A	BH070822-009	5240	swt
104	Cav 104A	BH070822-013	5244	swt
105	Cav 105A	BH070822-018	5249	swt
106	Cav 106A	BH070822-019	5250	sour
107	Cav 107A	BH070822-024	5255	sour
108	Cav 108A	BH070822-028	5259	sour
111	Cav 111A	BH070822-036	5267	sour
112	Cav 112	BH070822-040	5271	sour
Water	**from**	**ID #**	**Bottle #**	**Type**
101	C101	BH070822-003	5234	brine
102	Cav 102B	BH070822-007	5238	brine
103	Cav 103B	BH070822-011	5242	brine
104	Cav 104B	BH070822-015	5246	brine
106	Cav 106B	BH070822-021	5253	brine
107	Cav 107B	BH070822-026	5257	brine
108	Cav 108B	BH070822-030	5261	brine
111	Cav 111B	BH070822-038	5269	brine
112	Cav 112B	BH070822-042	5273	brine
Raw-1	raw water intake	BH070822-049	5280	raw water
Raw-2	raw water intake	BH070822-050	5281	raw water

EXPERIMENTAL METHODS

Physical Properties

Oil density and viscosity were measured over a small temperature range, from 20 to 30ºC using an Anton-Paar SVM 3000 Stabinger viscometer. Water sample density and pH were measured at 25ºC. Refractive index of each oil sample was measured at 20ºC using a GPR 11-37

automatic refractometer from Index Instruments. API gravity is calculated from the density at 20ºC using a standard temperature correction.

Chemical Characteristics

Acid and base numbers are measured by non-aqueous potentiometric titration using variations of the standard ASTM techniques (ASTM D664-01; ASTM D2896-98). A known amount of an organic base is used to force an endpoint for base number measurements, as first described by Dubey and Doe (1993). Adaptations to the acid number measurements, including spiking with stearic acid, are described in a recent paper by Fan and Buckley (2007).

Separation of crude oil into solubility fractions known as SARA (for saturates, aromatics, resins and asphaltenes) is based on the standard chromatographic method described in ASTM D2007-93. The method has been adapted to use an HPLC as described by Fan and Buckley (2002).

Interfacial Tensions

Interfacial tensions (IFT) between crude oil samples and their respective brines were measured using a pendant drop apparatus and software from DataPhysics (model OCA20 with SCA20 software). Measurement details are described in Buckley and Fan (2007). IFT of each of the oil samples was also measured with one of the raw water intake samples (Raw-1). The data were fit to an equation of the form:

$$\gamma = \gamma_{eq} + (\gamma_o - \gamma_{eq})e^{-t/\tau}$$

where γ is IFT (mN/m) with subscripts eq=equilibrium, and o=zero time or initial, t is time, τ is a characteristic time constant with the same units as time, t. Details and plots of the IFT measurements are in Sandia-ift.xls.

RESULTS

Table 2 summarizes the physical properties measured for oil samples. Those for water samples are in Table 3. Additional measurements and plots of density and viscosity as a function of temperature are in the spreadsheet (Sandia-summary.xls).

Table 2. Crude Oil Physical Properties

Oil	density at 20ºC (g/cm^3)	°API	viscosity at 20ºC (cP)	RI
101	0.8385	36.6	5.23	1.4707
102	0.8457	35.2	5.82	1.4748
103	0.8408	36.2	5.23	1.4717
104	0.8349	37.4	5.20	1.4693
105	0.8344	38.1	4.96	1.4693
106	0.8618	32.7	10.06	1.4867
107	0.8597	32.5	9.93	1.4858
108	0.8621	32.0	10.17	1.4870
111	0.8535	33.7	7.95	1.4804
112	0.8707	30.4	14.23	1.4911

Table 3. Water Properties

Water ID	pH	Density
101	5.6	1.2021
102	5.4	1.2021
103	5.8	1.2021
104	5.6	1.2021
106	5.9	1.2008
107	6.0	1.2008
108	5.8	1.2008
111	5.7	1.2008
112	5.5	1.2008
Raw-1	7.1	1.0031
Raw-2	7.4	1.0031

Comparison of RI, measured by the critical angle technique, and API gravity, calculated from the density measurement, provides a check on the internal consistency of these measurements. In addition, the values of RI and API gravity measured for this set of oil can be compared to previously measured results for 100 oils in the CO-Wet database, as shown in Fig. 1. All of these samples fall along the previously established trend of RI vs. API gravity. They span a small range of gravities; all but one is in the light oil range (API > 31.1°).

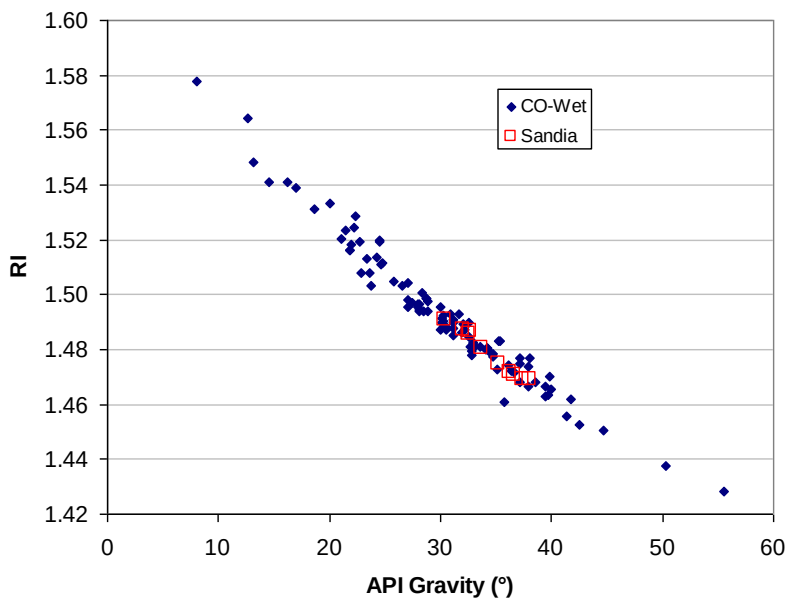

Figure 1. Comparison of RI and API gravity of the Sandia samples with the trend previously established by 100 crude oil samples in the CO-Wet database.

Oil sample acid and base numbers and SARA fraction data are summarized in Table 4. The range of acid and base numbers is fairly narrow compared to data in the CO-Wet database (c.f., Buckley and Wang, 2002). Sample 102 has a base number that is significantly higher than the other samples. All of the samples have at least a modest amount of asphaltenes.

Table 4. Crude Oil Chemical Properties

Oil	Acid #	Base #	Saturates	Aromatics	Resins	n-C6 Asphaltenes
	mg KOH/g oil		wt %			
101	0.30	1.56	66.3	19.9	12.6	1.2
102	0.49	2.55	62.2	19.4	16.7	1.7
103	0.43	1.71	64.3	21.4	13.5	0.9
104	0.19	1.47	64.0	21.9	13.0	1.2
105	0.20	1.47	64.5	20.5	13.9	1.1
106	0.28	1.44	59.5	21.3	16.2	3.1
107	0.28	1.46	58.2	21.6	16.8	3.4
108	0.29	1.50	58.3	21.6	17.0	3.1
111	0.43	1.57	59.7	23.8	14.1	2.4
112	0.30	1.65	56.3	21.8	18.9	3.0

Table 5 summarizes the equilibrium interfacial tension data. Each oil was tested with the brine from the same source, except sample 105 for which there was not a corresponding brine sample. Brine 104 was used instead. In all cases, the IFT measured with the raw water sample was lower than that measured with the brine. The difference was 5.5 mN/m on average. Sample 102, which has the highest base number, has the lowest values of IFT with both brine and raw water. Meaningful statistics relating oil properties to IFT cannot be obtained with this small data set, especially since the oils are fairly similar in properties.

Table 5. Equilibrated Interfacial Tensions

Oil	IFT-brine	IFT-raw	ΔIFT
	mN/m		
101	26.5	21.3	5.3
102	22.0	19.0	3.0
103	28.0	20.0	8.0
104	27.0	20.0	7.0
105	26.5*	19.5	7.0
106	28.0	24.5	3.5
107	26.5	20.0	6.5
108	26.5	21.5	5.0
111	27.5	24.0	3.5
112	27.0	21.0	6.0

* measured with 104 brine

REFERENCES

ASTM D664-01: "Standard Test Method for Acid Number of Petroleum Products by Potentiometric Titration," *ASTM* (1989).

ASTM D2007-93: "Standard Test Method for Characteristic Groups in Rubber Extender and Processing Oils by the Clay-Gel Adsorption Chromatographic Method," *ASTM* (1993).

ASTM D2896-98: "Standard Test Method for Base Number of Petroleum Products by Potentiometric Perchloric Acid Titration, *ASTM* (1998).

Buckley, J.S. and Fan, T.: "Crude Oil/Brine Interfacial Tensions," *Petrophysics*, (2007) **48**, 175-185.

Buckley, J.S. and Wang, J.X.: "Crude Oil and Asphaltene Characterization for Prediction of Wetting Alteration," *J. Pet. Sci. Eng.* (2002) **33**, 195-202.

Dubey, S.T. and Doe, P.H.: "Base Number and Wetting Properties of Crude Oils," *SPERE* (Aug. 1993) **8**, 195-200.

Fan, T. and Buckley, J.S.: "Rapid and Accurate SARA Analysis of Medium Gravity Crude Oils," *Energy & Fuels* (2002) **16**, 1571-1575.

Fan, T. and Buckley, J.S.: "Acid Number Measurements Revisited," paper SPE 99884 presented at the 2006 SPE IOR Symposium, Tulsa, 22-26 April (accepted for publication in SPEJ, 2007).

DISTRIBUTION

External Distribution

Electronic copies to:

Wayne Elias (wayne.elias@hq.doe.gov) for distribution to DOE SPR Program Office, Washington, DC

Diane Willard (diane.willard@spr.doe.gov) for distribution to DOE and DM SPR Project Management Office, New Orleans, LA

Sandia Distribution

Print copies to:

5	MS0706	David Lord	6912
5	MS0750	Carolyn Kirby	6913

Electronic Copies:

MS0899 Technical Library, 9536 (electronic copy)

[This page intentionally blank]

Sandia National Laboratories